Master Thesis, Department of Geosciences

Zircon age distributions in sediments from eastern Iceland: continental material along the SW-extension of the Jan Mayen Ridge

Daniel Angler Valrygg

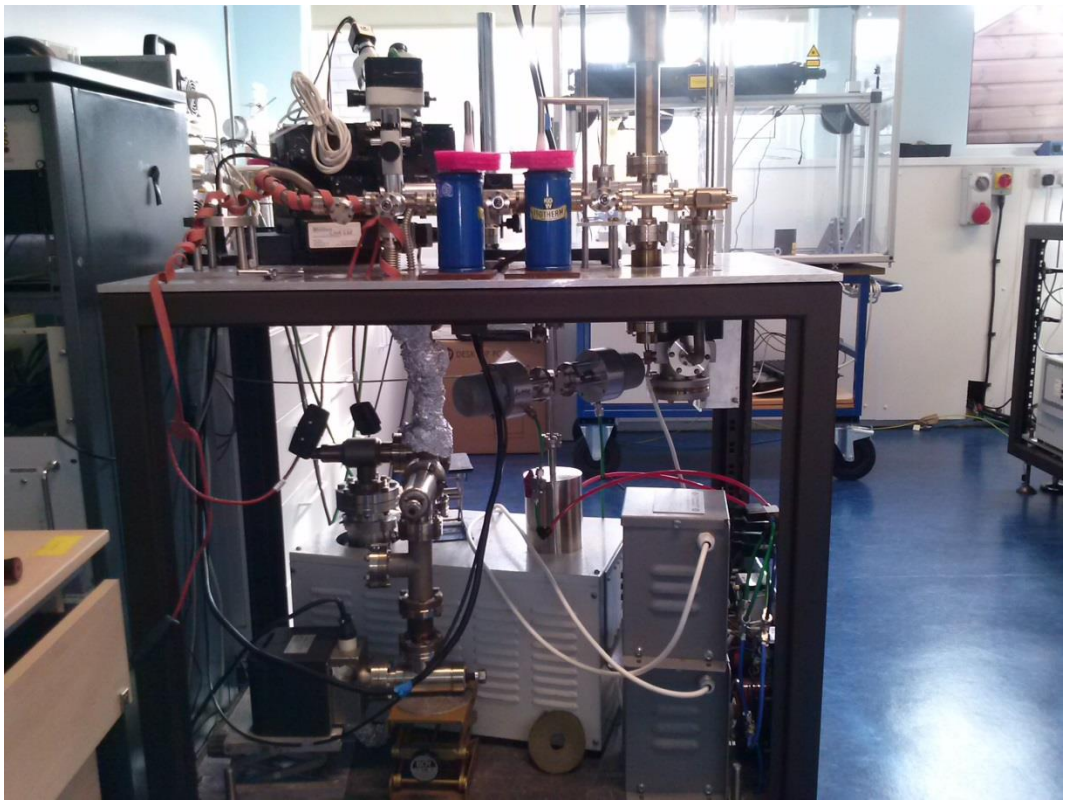

UNIVERSITY OF OSLO

FACULTY OF MATHEMATICS AND NATURAL SCIENCES

Zircon age distributions in sediments from eastern Iceland: continental material along the SW-extension of the Jan Mayen Ridge

Daniel Angler Valrygg

Master Thesis in Geosciences

Discipline: Geology

Department of Geosciences

Faculty of Mathematics and Natural Sciences

University of Oslo

02.06.14

Tutors: Professor Reidar G. Trønnes and Fernando Corfu

This work is published digitally through DUO – Digitale Utgivelser ved UiO

http://www.duo.uio.no

It is also catalogued in BIBSYS (http://www.bibsys.no/english)

Acknowledgements

I have always been a great fan of science, and started at quite an early age to show an urge for learning. I started with a magnifying glass to explore the world around med before I could write and read, got my first microscope (my top wish that Christmas) at the age of twelve, and ended up with writing a thesis in geology. I am ever so grateful for this experience, even though it has been frustrating at times. The experience of writing and learning about the mysterious zircon grains has certainly showed me what I believed science to be all about to be true. It is uncertain, it is interesting and it takes a lot of work.

First of all I would like to thank my main supervisor, Reidar G. Trønnes for the opportunity to join up on such a fascinating project. The time you have spent teaching me about Iceland and guiding me through the thesis must be quite an amount of time. Without your guidance, there would not be much of a thesis. My second supervisor Fernando Corfu deserves a special thank you for his help to teach me about the finer details about U-Pb dating, and for his patience even when I do mistakes. His stories and conversations about science (and football!) have a value to me that cannot be measured by a grade. I would never think that an excursion could be that interesting, but the trip to Iceland certainly was. I now know that if I can survive the Icelandic killer-birds, then I can survive anything. A thank you to Fin Stuart at SUERC for his help and guidance during my stay in Scotland, and especially for showing me his favourite pub! I will always appreciate the laughs and interesting talks after a couple of beers.

I would also like to thank Margareth and Terry Donnelly, for opening up their home and making me feel so welcome at my stay in Scotland. Berit Løken Berg deserves a thank you for all your help during sample separation. Your good mood is very contagious.

I would further like to thank my friends at the University of Oslo, for all the good times and laughs.

Last, but not least, a very special thank you to Eva H.Fritzell, for always being a great support. Your hugs when I have been tired have been of great motivation.

Abstract

Iceland is the result of plume-ridge interaction on the boundary between the North American plate and the Eurasian plate. Preliminary findings of Precambrian xenocrystic zircon grains in the Öræfajökull area might indicate an underlying extension of the JMR beneath SE Iceland (Foulger, 2006; Paquette et al., 2007, Torsvik et al., in prep). This hypothesis was partly motivated by, and could explain the unique isotope geochemistry in the SE Iceland, previously attributed to an EM2 mantle signature (Prestvik et al., 2001). In this study river sediments from a wider area around the Öræfajökull volcano were sampled and washed on-site for heavy mineral concentration, before zircon selection and U-Pb dating by ID-TIMS at the University of Oslo, yielding no Precambrian zircons. Most of the remaining sample material from 2003 that had previously yielded Precambrian xenocrysts was also crushed, milled, separated and handpicked without further indication of Precambrian zircon grains.

A firm conclusion identifying the reason(s) for the lack of Precambrian zircons in the new samples and the re-examined additional fractions of the 2003 samples cannot be reached, but several alternatives are discussed. I consider laboratory contamination as plausible; whereas in-situ contamination of river sand and hyaloclastite material in SE Iceland by wind transportation, ice rafting and anthropogenic sources seem less likely. The failure to detect more Precambrian zircon xenocrysts in this study does not exclude the possibility that the original SE Iceland xenocrystic zircon population was derived from assimilation of continental crust of an extended Jan Mayen Microcontinent (JMM) under SE Iceland.

Four of the Precambrian xenocrysts dated prior to this thesis were also measured for its amount of helium at SUERC in Scotland. This was done in an effort to investigate if the Precambrian zircons lost He in the hot environment of crustal xenotlith assimilation in the recent magma chambers and conduits. The Precambrian xenocrysts, however, gave (U-Th)/He ages that were similar to their U-Pb ages.

This result motivated a further investigation of the correspondence between (U-Th)/He ages and U-Pb ages in a selection of samples of Precambrian rocks from southern Norway. The

samples were chosen to reflect various tectonic and thermal regimes in order to study the effect of differential helium retention in zircon. The consistent finding that the (U-Th)/He ages were reset by younger thermal processes (mostly Caledonian and Oslo Rift overprinting) in all these samples, combined with similar results indicating younger thermal effects from available fission track data, might indicate that the Precambrian xenocrysts from SE Iceland are unlikely products of contamination by zircons from southern Norway (or Norway in general). In contrast, some of the published fission track data from Finland, eastern Sweden and Greenland give ages that are Precambrian. Based on a new synthesis by Torsvik et al. (in prep.), indicating that the JMM was derived from the East Greenland margin, it seems conceivable that Precambrian crustal zircons, as well as the unique geochemical anomaly centered in the southern part of the Eastern Volcanic Flank zone, are derived from these regions.

This thesis is the first to present (U-Th)/He ages from zircons in the Oslo Region, Bamble and Telemarkia terranse, and Hardangervidda. The thesis is also the first to report U-Pb ages from an orthogneiss in Nevlunghavn (together with unpublished data from F.Corfu), giving an upper intercept on the Concordia curve at 1552.4 ±6.0 Ma and a lower intercept at 302 ±41 Ma. The lower intercept is thought to reflect lead loss during the emplacement of the Larvikite plutonic complex.

Table of content

1. Introduction

The isotope geochemistry of the rock suite of the Öræfajökull central volcano is characterized by high $^{87}Sr/^{86}Sr$ ratios and high $^{207}Pb/^{204}Pb$ and $^{208}Pb/^{204}Pb$ at intermediate $^{206}Pb/^{204}Pb$ ratios (Prestvik 2001, Kokfelt et al., 2006, Debaille et al., 2009). The isotopic composition is unique in the NE Atlantic and may be ascribed to an EM2 mantle source signature or a mantle source enriched in pelagic sediments (Prestvik, 2001; Kokfelt et al., 2006). Torsvik et al. (in prep), however, suggest that the unique signature is caused by contamination of basaltic melts with continental crust. That study was based on preliminary investigations, reporting (in abstract form only) the presence of Precambrian and late Paleozoic to Mesozoic zircons in southeast and northeast Iceland (Schaeltegger et al., 2002; Amundsen et al., 2002; Paquette et al., 2006). Xenocrystic zircon grains found in Mauritius might be associated with several micro-continental fragments (e.g. Torsvik et al., 2013), and shows that zircons may survive in basaltic melts and transport to the surface.

Kumar et al., (2007) reports a Moho depth of near 50 km in the SE and NW- part of Iceland (figure 1) in contrast to previous studies reporting the greatest depth in the central part of Iceland (e.g. Foulger 2006).

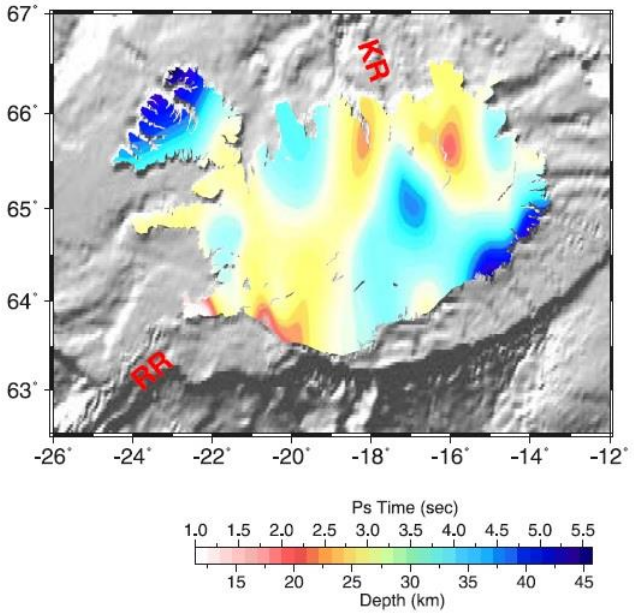

Figure 1. Contour map of the Moho depth of Iceland, showing the greatest Moho depth in the SE and NW of Iceland. Reykjanes Ridge (RR) and Kolbeinsey Ridge (KR) are partly visible. Figure from Kumar et al. 2007.

The presence of continental material beneath the south eastern part of Iceland could explain the mentioned "Icelandic anomalies", and the proximity to the Jan Mayen microcontinent (Jan Mayen Ridge; JMR) raises the question of whether the JMR extends beneath the eastern part of Iceland (Foulger, 2006; Paquette et al., 2007, Torsvik et al., in prep.). Torsvik et al., (in prep.) model the Snæfell and Öræfajökull basalts as a mixing trend by contamination of Hofsjökull basaltic magmas with 1-6 % continental crust.

The basis for the current investigation includes the preliminary reports of Schaltegger et al. (2002) and Amundsen et al. (2002) and a new collection of zircons extracted from river sediments and a hyaloclastite unit sampled in the area south of Öræfajökull in 2003 (by R.G. Trønnes) and separated and dated in Oslo in 2003-2004 and 2013 (prior to the start of the current project). The 2003-samples covered a hyaloclastite unit and sand from a small stream near Hnappavellir and the Stigá and Gljúfúrsá glacial rivers (50-100 m upstream from the main road bridges). The heavy mineral concentrates (separated in 2003 by M. Schjoldager, working for H.E.F. Amundsen) contained various amounts of zircon grains. Dating selected grains (based on appearance) revealed four Precambrian grains in 2004 and another four Precambrian grains in 2013 (U-Pb-geochronology by Fernando Corfu).

The current study was designed to further investigate and verify the presence and distribution of Precambrian xenocrystic zircons in river sediment samples from the Öræfajökull area. Sampling in a wider geographical area around the Öræfajökull central volcano might potentially reveal a more closely defined distribution of xenocrystic zircons. One of the samples was collected at elevations above the Holocene upper marine limit, in order to address the possibility of zircon contamination of sedimentary units by ice-rafted sand and gravel, e.g. from east Greenland.

The sampling and analyses of Öræfajökull material for the current investigation included:

a) On-site heavy mineral washing in several selected rivers in the Öræfajökull area.
b) Mineral separation and U-Pb age determination of selected zircon grains by ID-TIMS at the University of Oslo.

Because this investigation only resulted in young zircons (except one 30 Ma old grain, see the results and discussion sections), it was decided to investigate most of the remaining unprocessed parts of the sample material from 2003. This included the hyaloclastite tuff unit (SAL-779) and the corresponding pillow-lava unit (SAL-769) that had to be crushed and milled before separation (processed by D.A. Valrygg), as well as the Stigá and Gljúfúrsá glacial river samples (processed by F. Corfu).

The second part of the thesis was motivated by an effort to understand the provenance of the Precambrian zircon grains recovered from east Iceland prior to this thesis. In May-June, 2013 the amount of He had been measured at SUERC in Scotland for a selection of carefully chosen zircons, including a few with similar appearance to the grains that had previously given Precambrian ages. The grains were then dissolved at the University of Oslo for determination of the amounts of U, Th and Pb and the isotope ratios. The dated grains gave (U+Th)/He-ages (hereby referred to as U-He age) that are broadly similar to their U-Pb-ages, for both the young and old age groups analysed. The findings are given in the result section and include SB1, GB1, HVRT1 and SAL 779. These results have several potential implications and form the basis for the second part of the study.

1) If the Precambrian zircon grains from east Iceland were scavenged from old crust beneath the island, and heated up to the temperature of the basaltic melt during volcanic processes, several hundred degrees higher than the blocking temperature of He (i.e. retention of He in zircon) at c. 200°C, then most of the radiogenic He should theoretically be lost, yielding a low age. Since that is not the case, the heating during the volcanic process cannot have been sufficiently high or long to cause complete outgassing of the grains. By dating zircon grains (see C-06-3 in the result section) from Precambrian gneiss xenoliths within the southern larvikite pluton in the eastern part of the Oslo rift, it could be tested if He in zircons exposed to a high thermal gradient would yield a positive correlation or not. Would these zircons also preserve an old U-He age? In spite of Caledonian Permian overprints and later Mesozoic sedimentation and differential uplift, would positive correlating He ages also be expected in the Oslo region, more peripheral to the larvikite plutons?

2) The alternative is that the grains recovered from the Öræfajökull area are not from Iceland, but derived from other sources. One possibility that needs to be considered is that the zircon

grains could be contaminants from sample preparation. The samples were processed in Oslo, and the U-Pb ages of the Precambrian zircons in the Icelandic samples (1.5-1.0 Ga) match those of basement in the Oslo region. Could it be possible to rule out certain regions (e.g. Oslo region or East Greenland) as the source of the xenocrysts, by seeing how closely the U-He and U-Pb ages from these regions match up?

In the second part of the thesis, I therefore investigated the corresponding U-He and U-Pb ages of zircons from a selection of Precambrian and Permian rocks from South Norway. The samples include a gneiss from Gjersjøen (about 1512 Ma) 12 km east of the Oslo Rift, a Precambrian crustal xenolith in the larvikite at Nevlunghavn in the Vestfold graben (about 1552 Ma), the larvikite from the same area (292-297 Ma), a porphyritic gneiss from Brunkeberg in the Bamble complex (about 1553 Ma), a granite from Finse (about 990 Ma) and Kvitenut (about 1627 Ma) at Hardangervidda.

The U-He ages provides an indication of the thermal evolution of southern Norway, given that this thesis is the first to report such U-He ages. Fission track (FT) ages are provided by Rohrman et al (1994) for apatite, zircon and titanite from the Oslo Region, Telemark and Bamble, giving indications to the thermal history of the region. How would the He ages provided by this thesis fit into the thermal evolution of the Oslo Region and surrounding areas? Gjersjøen in Kolbotn, which lies just outside of the Oslo rift, provides a good opportunity to see if heat dissipation from within the rift would affect the rocks just outside the rift sufficiently to diffuse out helium, or even if later processes would reset the He age. Samples from Finse and Kvitenut at Hardangervidda were chosen as a part of the study to see if zircons from these rocks would show He ages younger than the Caledonian Orogeny, and how well these ages would compare with fission track data by e.g. Hendriks et al. (2007).

The practical aspects of the second part of the thesis included:

a) Measurement of the amount of He for selected grains at Scottish Universities Environmental Research Centre (SUERC).

b) Dissolving and measurement of the selected zircon grains for the amount of U and Th and Pb isotope ratios to determine both He age and Pb age by ID-TIMS at the University of Oslo.

2. Regional setting

2.1 Iceland

The Iceland plateau in the shallowest part of the north Atlantic (Ocean), covers an area about 350 000 km^2. Approximately 30% is visible above sea level; the reminder of the area forms a 50 – 200 km wide shelf surrounding Iceland (e.g. Gudmundsson, 2000 and references therein). The plateau is situated at the junction between two large submarine structures, The Mid Atlantic Ridge and the Greenland-Iceland-Faeroe Ridge (figure 2). Iceland is (considered to be) a fascinating example of tectonism and volcanism resulting from plume-ridge interaction (e.g. Hardarson et al., 1997; Allen et al., 2002; Thordarson and Larsen, 2007) on the boundary between the North American plate and the Eurasian plate.

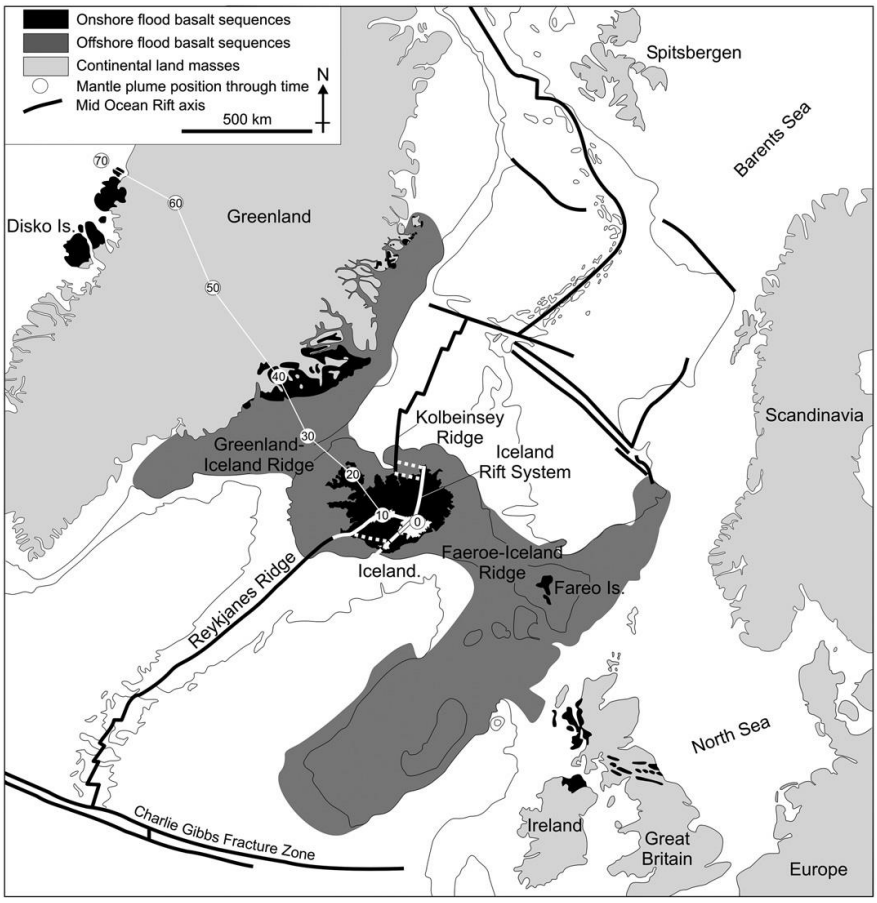

Figure 2. Showing the two large submarine structures, The Mid Atlantic Ridge and the Greenland-Iceland-Faeroe Ridge. The solid black line is the axis of the Mid Atlantic ridge. Figure from Thordarson and Larsen, 2007.

The North Atlantic Igneous Province (NAIP) is one of the largest Large Igneous Provinces (LIP) and covers over 2000 km^2, from Baffin Island and West Greenland in the west, the British Isles in the east, and Hold with Hope in NE Greenland in the north. The NAIP was formed from the Iceland Mantle Plume, where Iceland is the only part still active (e.g. Saunders et al., 1997).

The Iceland Mantle Plume has been active the last 62 million years and the bulk of the magmatic activity occurred in two main phases. The first phase erupted through and onto continental crust, lasting 2 – 4 million years, while the second phase began with the onset of plate breakup at 55 Ma and lasted until present day Iceland (e.g. Saunders et al., 1997). At c. 20 Ma the Iceland plume positioned below the spreading axis (Torsvik et al., 2001) and the center of the mantle plume is today presumed to be located beneath the NW part of the Vatnajökull icecap (Martin and Sigmarsson, 2010; Martin et al., 2011).

The North American and Eurasian plate are currently moving apart with a half-spreading rate of about 1 cm / year (e.g. Torsvik et al., 2001; Allen et al., 2002; Foulger, 2006; Martin et al., 2011). The magnetic lineament pattern and ocean basin width southwest of Iceland indicate a nearly constant spreading rate since the ocean basin opening at 55 Ma. The oldest basaltic rocks dated in Iceland, Miocene basalt, are 16Ma in the NW, 15Ma in the NE and 13 Ma in the E (Hardarson et al., 1997). With a simple spreading axis in the middle and a plate velocity of 1 cm/a (10km/Ma), the expected distance between the outermost and oldest localities in the NW and NE would therefore be 310 km, in comparison with the actual distance of 450 km. This contrast with a total width of 500-600 km for the 55 Ma old ocean crust SW of Iceland, formed along the single Reykjanes Ridge with an average half-spreading rate of 10 km/Ma. A crustal accretion model with major transform movements, rift jumps and periods with spreading along at least two semi-parallel rift zones can readily explain the excessive width (W-E-extension) of Iceland (e.g. Martin, 2011). The crustal thickness models of Allen et al. (2002) and Foulger (2006) indicate variations from about 15 km on the Reykjanes Peninsula to more than 40 km north of Vatnajökull. A receiver function study by Kumar et al. (2006) has resolved more detailed variations with the greatest crustal thicknesses in the Askja area in

the east-central interior (40 km), along the SE coast from Höfn to Reydarfjördur (42-48 km) and at the Isafjördur peninsula in the NW (38-43 km).

The interaction of the Iceland Plume with the Mid-Atlantic spreading ridge (MAR) system, The Kolbeinsey Ridge (KR) in the north and the Reykjanes Ridge (RR) in the south, is most easily recognized by the active volcanic zones (neovolcanic zones) and belts (figure 3), and Iceland's elevation above sea level (Thordarson and Larsen, 2007).

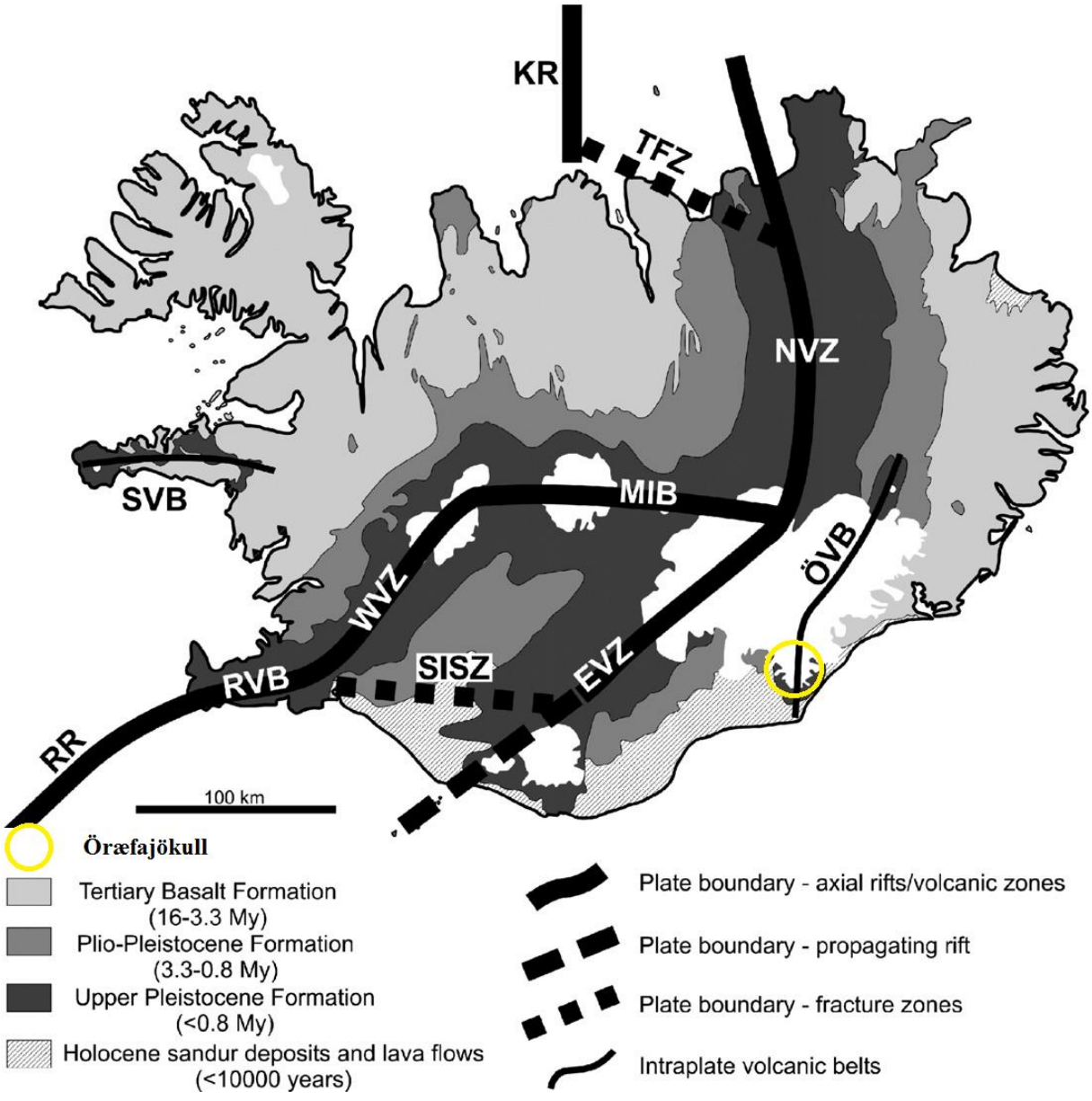

Figure 3. A simple map showing the principal elements of the geology in Iceland, outlining the major subdivision of rock formations, the main fault structures and volcanic zones and belts. RR, Reykjanes Ridge; SISZ, South Iceland Seismic Zone;

EVZ, Eastern Volcanic Zone; WVZ, West Volcanic Zone; SVB, Snæfellsnes Volcanic Belt; MIB, Mid-Iceland Belt; ÖVB, Öræfi Volcanic Belt; NVZ, North Volcanic Zone; TFZ, Tjörnes Fracture Zone; KR, Kolbeinsey Ridge. Figure from Thordarson and Larsen, 2007.

The KR trends sub-perpendicular to the spreading vector, with a crustal thickness exceeding that of a normal mid oceanic crust by 1.0 – 1.5 km. The RR is an oblique spreading ridge, consisting of axial volcanic systems (fissure swarms) in an en echelon arrangement. The 30-60 km wide Icelandic rift zones with 2-4 sub-parallel and en echelon volcanic systems are the sub-aerial expressions of spreading near the current plume center. The rift zone volcanic systems have life times of 0.5-1.5 Ma (Thordarson and Larsen, 2007) and develop from an early fissure swarm to a fissure swarm associated with a productivity center: a central volcano. Many of the volcanoes develop caldera structures associated with eruptions of more evolved magmas. The volcanic systems in the non-rifting flank zones lack fissure swarms.

Three main segments make up the neovolcanic zone: The North Volcanic Zone (NVZ), The West Volcanic Zone (WVZ) and the East Volcanic Zone (EVZ) (figure 3). The Reykjanes Volcanic Belt (RVB) is the southernmost (southwest) segment of the MAR in Iceland, joining up with the WVZ. Further north the WVZ bends eastward towards the NVZ, through a transform fault system (Martin and Sigmarsson, 2010), the Mid-Iceland Belt (MIB, or Mid-Iceland volcanic zone as described by Martin and Sigmarsson, MIVZ). The NVZ extends from north coast towards the MIB, while the EVZ, a young rift in making that will eventually reach the RR, extends from the southern part of NVZ to the south coast (e.g. Thordarson and Larsen, 2007, Gudmundsson, 2007). The volcanic systems in the rift zones are influenced by the rifts tectonic forces, preventing them from developing edifices to a great height.

There are three active off-rift or flank zones: The Snæfellsnes Volcanic Belt (SVB) (or Snæfellsnes Volcanic Zone (SNVZ)) is situated in the western Iceland and may represent a continuation of a leaky transform belt. The Öræfi Volcanic Belt (ÖVB) which may represent an embryonic rift runs from Snæfell in the northeast to Öræfajökull in the southeast. The Southern Volcanic Zone (SVZ) is a propagation of the EVZ, ending in southern Iceland (Martin and Sigmarsson, 2010). The volcanoes in the flank zones are less affected by tectonic forces and will therefore build up much larger and competent stratovolcanic edifices. The rocks produced in the flank zones tend to be of the alkalic series (Jonasson, 2007) while the

volcanic flank zones have transitional alkali to tholeiitic composition (Prestvik et al., 2001).

The Tjörnes Fracture Zone (TFZ) off the north coast, is a leaky transform fault, 120 km long and 70 km wide WNW trending, connecting the KR with the North Volcanic Zone (NVZ). The TFZ consist of three seismically active lineaments of which the main section is the Húsavík-Flatey Fault, a well-developed dextral strike slip fault (Gudmundsson, 2000). The South Iceland Seismic Zone (SISZ), a southern complement of TFZ is a zone of complex faulting, linking the southern ends of the parallel West Volcanic Zone (WVZ) and East Volcanic Zone (EVZ). The SISZ is 70 km long and 10-20 km wide, with almost continuous seismic activity superimposed on intermittent episodes of large activity. These episodes with a few earthquakes of magnitude 5-7 may last for less than 10 years and are separated by about 100 years. The TFZ and the SISZ are both ocean-ridge discontinuities formed as a consequence of shear-stress concentrations between nearby ends of ocean-ridge segments (Gudmundsson, 2007).

The Icelandic rocks are approximately 10% silicic, which is unusually within the oceanic crust (Jonasson, 2007), while most of Iceland is basaltic (90%), (e.g. Gunnarsson et al., 1998). The abundance of intermediate rocks are rare, and have been showed to be formed by hybridization or mixing (Jonasson, 2007). The volcanic rocks are therefore compositionally bimodal, separating the basaltic and silicic compositions. The formation of silicic rocks have great implication in understanding the earths early and ongoing history, as it may give insight on the geochemical processes of continent formation (Jonasson, 2007 and references within). The silicic rocks are found mostly within central volcanoes in both the rift and flank zones.

Two models try to explain the origin of silicic magmas in Iceland. The first model favors fractional crystallization of a mafic magma (e.g. Prestvik et al., 2001; Selbekk and Trønnes, 2007; Flude et al., 2008) while the second model favors partial melting of hydrothermally altered crust (e.g. Gunnarsson et al., 1998; Jonasson, 2007; Bindeman et al., 2012). Jonasson (2007) argues that one way to test the different models is to consider if the Icelandic rocks are formed by near liquidus fractionation (the former model), or near solidus fractionation (the

latter model), concluding that near solidus fractionation best explains the formation of silicic rocks.

Martin and Sigmarsson (2007, 2010) argue for a combination of fractional crystallization and partial melting by introducing a link between the mode of silicic magma formation and the thermal state of the crust. Crustal anatexis dominate the formation of rhyolites in the rift-zones while the off-rift zones are formed by fractional crystallization (Martin and Sigmarsson, 2007, 2010).

2.2 Öræfajökull

Located at the southern end of the Öræfi Volcanic Belt, ca 50km east of the eastern volcanic zone, the Öræfajökull stratovolcano is the only Icelandic volcano that has been active in recent time without being tectonically related to the active volcanic rift zones (Prestvik, 1985; Sigmarsson et al., 1992). The NE-SW- trending off-rift volcanic zone (ÖVB) runs 120km northward, ending in the Snæfell volcano. The central volcano lies unconformably on uplifted and eroded Tertiary basalt and is the largest Icelandic volcano, reaching an altitude of 2119 m a.s.l (Larsen et al., 1999; Prestvik, 2001; Selbekk and Trønnes, 2006). With its 14 valley glaciers cutting radially southwest and southeast- wards, the Öræfajökull forms the south eastern part of the larger Vatnajökull icecap. The volcano is ice covered (figure 4) and has an elongate 4-5 km diameter ice-filled summit caldera containing ice up to 500 m thick (McGarvie, 2008).

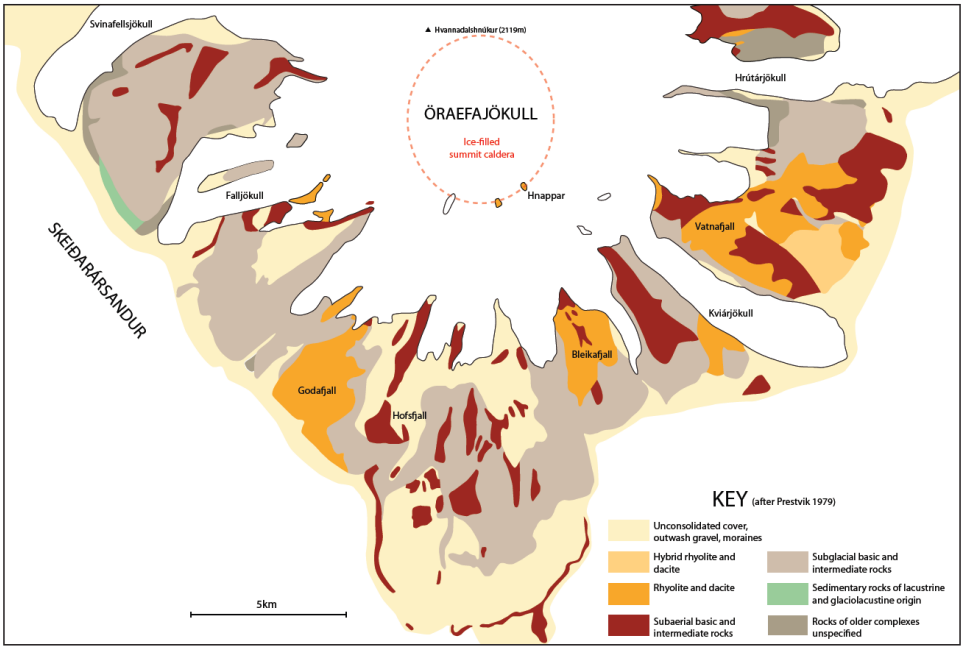

Figure 4. Geological map of Öræfajökull. Figure from Walker, 2011.

The Öræfi stratovolcano eruptive deposits are dominated by sub-glacially erupted hyaloclastite units with pillow lava and tuff ranging in composition from basalt through hawaiite, mugearite, benmorite, trachyte to rhyolite (Prestvik, 1985, 2001; Selbekk and Trønnes, 2006). Only a small number of exposures, however, have been found (figure 5) (Stevenson et al., 2006; Walker, 2011). Prestvik (1985) originally characterized the rock series as tholeiitic, and although the author mentioned its transitional character, he later refers to IUGS classification and classifies the series as sodic alkaline ($Na_2O - 2.0 \geq K_2O$). The low MgO- content ($MgO \leq 6.15$ wt %) of the basic rocks (basalts and hawaiites) of Öræfajökull indicates that these rocks are quite evolved and further distinguishes the rocks from the active rift zones (Prestvik, 2001).

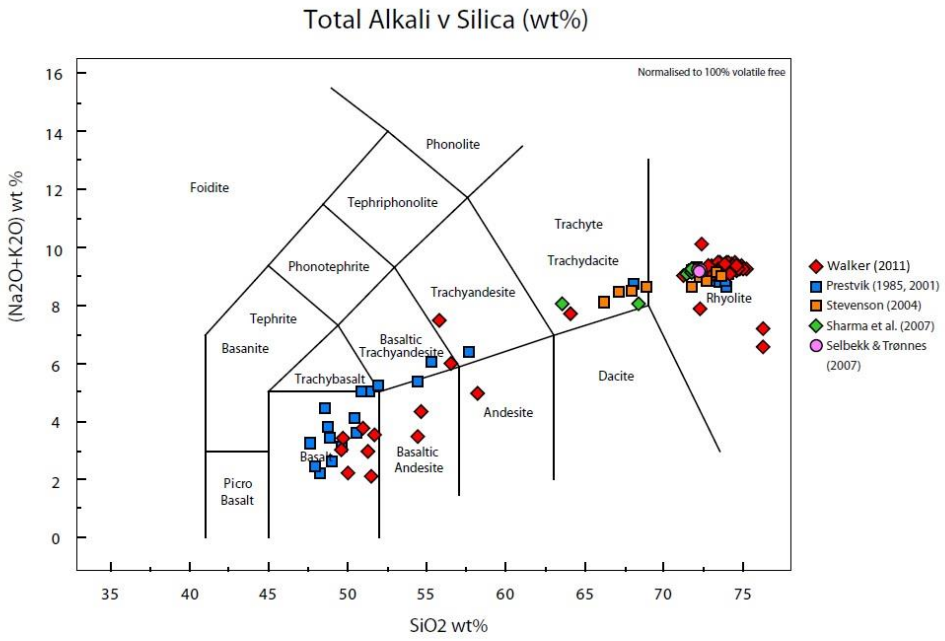

Figur 5. Total Alkali v Silica (TAS) diagram showing published Öræfajökull major element data. Figure from Walker, 2011.

Compared to Icelandic rift basalts, the Öræfajökull rocks are enriched in $^{207}Pb/^{204}Pb$ and $^{208}Pb/^{204}Pb$ isotope ratios (Prestvik, 2001, Kokfelt et al., 2006), and have the highest $^{87}Sr/^{86}Sr$ ratios (0.7037) in both basalts and rhyolites (than observed for any other Icelandic rocks) (e.g. Prestvik, 2001; Sigmarsson et al., 1992; Condomines, 1983, Debaille et al., 2009).

In order to explain the high Sr-ratios, Sigmarsson et al. (1992) considers sea spray, infiltration by seawater and contamination of the magma by marine carbonates as potential agents. Prestvik (2001), however, argue that the high Pb and Sr isotope ratios are better explained by an EM2-type mantle component. The basic, intermediate and silicic rocks from Öræfajökull all show anomalously high Sr isotope ratios, leading Prestvik (2001) to argue that all rocks most likely formed from a common enriched source and that the rhyolites and other evolved rocks formed by various degrees of fractional crystallization of basic melts. The anomalous Pb data from both basic and more evolved rocks also points to a common source(s) for all young rocks, different from that of the old basalts (Prestvik, 2001, Kokfelt et al., 2006).

The lack of amphibole in Iceland and an elevated K_2O content in Icelandic rhyolites and basalts compared to the usual mid-ocean ridge setting, indicate a relatively dry melt. The low water content of the flank zone magmas is consistent with a lack of extensive geothermal activity in the flank zone central volcanoes, leading to a more extensive fractional crystallization accompanied by latent heat dissipation without bringing the wall rocks to their solidus temperature (Selbekk and Trønnes, 2006). The extreme phenocryst compositions of fayalite ($Fa_{99,7}Fo_{0,3}$) and hedenbergite ($Wo_{44,7}En_{2,6}Fs_{52,7}$) in the 1362 tephra further indicates fractional crystallization.

By comparing Ti and Hf concentrations from zircons from four different volcanoes: Askja (on-rift), Torfajökull (propagating rift-tip), Hekla (transitional to rift) and Öræfajökull (off-rift), Bindeman et al. (2011) are able estimate the zircon growth temperatures for the different tectonic settings (figure 6).

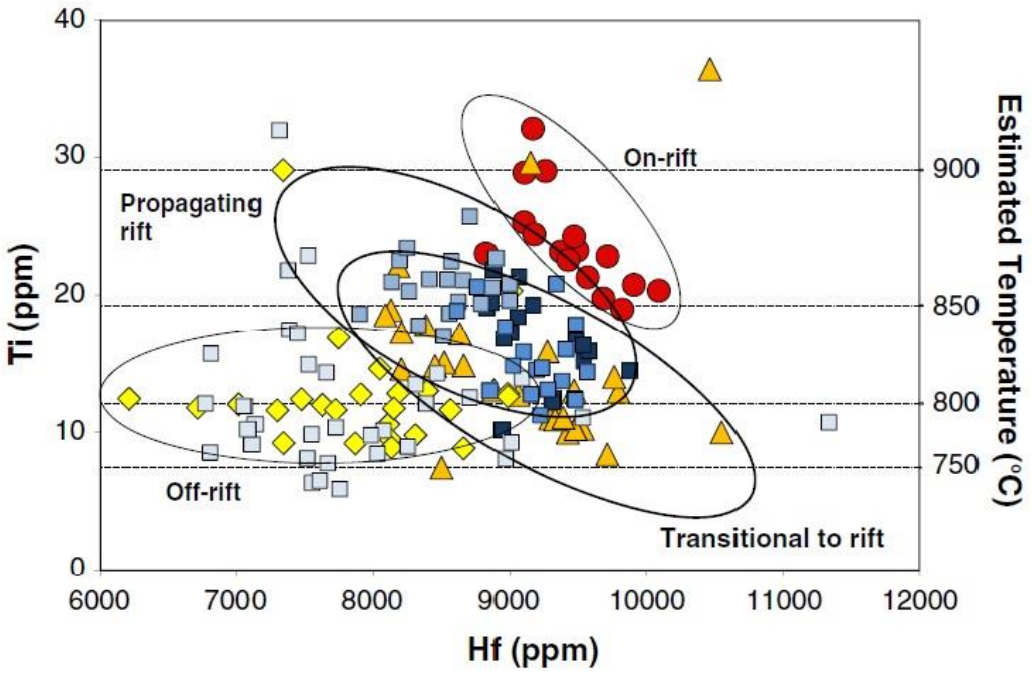

Figure 6. Titanium vs Hafnium concentrations for the different tectonic settings. See text for detailed description. Figure from Bindeman et al., 2011.

The Ti and Hf concentrations suggest that the zircon growth temperatures are higher in magmatic systems nearest to the active rift zone, consistent with Prestvik (2001) and Selbekk

and Trønnes (2006) suggestion on fractional crystallization dominating in the off-rift zones. Sigmarsson and Martins (2010) argue that the geothermal gradient appear to control the petrogenetic processes of silicic magma formation in Iceland.

The $\delta^{18}O$ values for the Öræfajökull rocks varies from 5.0‰ for a basalt (Sigmarsson et al., 1992), 5.0 – 5.6 ‰ for basic rocks and 4.8 – 6.2 ‰ for fresh intermediate silicic rocks (Prestvik, 2001), and 6.11‰ for a rhyolite (Condomines, 1983), which all are considerably higher than those observed in the Icelandic rift system. The origin of low $\delta^{18}O$- basalts closer to the active rift system is thought to reflect contamination of mantle derived melts by hydrothermally altered crust (e.g. Oskarsson et al., 1981, Gunnarsson et al., 1998). These rocks could have originally been produced in the rift zones and later buried by isostatic subsidence (Oskarsson et al., 1981 and reference therein).

The relatively homogenous composition ($\delta^{18}O$, Sr and Pb isotope ratios) ranging from basalts to rhyolites, indicate that a possible contamination with continental crust was deep-seated and affected the basaltic parental magmas.

Öræfajökull has erupted twice in historical times, first a large plinian eruption in 1362 AD and later a small benmoreitic eruption in 1727 AD (Larsen, 1997; Selbekk and Trønnes, 2006; Sharma et al., 2008). The 1362 eruption produced at least 10 km^3 silicic tephra, corresponding to 2km^3 dense rock equivalent (DRE) and is thought to be Iceland`s most voluminous explosive eruption to have occurred in historical times (e.g. Larsen, 1997). The eruption started in June and proceeded in three main phases (Sharma et al., 2008). The eruption and its associated glacial lahars (jökulhlaups – glacier outburst floods) caused widespread damage and destroyed at least 30 farms (Thorarinsson, 1958). The volume of the 1727 eruption was smaller than the 1362 eruption, and probably did not exceed 0.2 km^3 of tephra (Thorarinsson, 1958). The compositional homogeneity of the phenocrysts of the 1362 tephra are “remarkably homogenous” (Selbekk and Trønnes, 2006), indicating a uniform and well equilibrated magma chamber.

2.3 The Baltic shield

The Precambrian Baltic shield extends across Norway, Sweden, Finland and north-western Russia. The continental crust was formed between 3.5 and 1.5 Ga during four periods of orogenic activity (Gaál and Gorbatschev, 1987), the earliest being the Saamian Orogeny. The Baltic shield is oldest in the northeast and gets progressively younger towards the southwest. This geochronological zonation reflects the formation of continental crust during the Lopian orogeny from 2.9-2.6 Ga, the Svecofennian orogeny from 2.0-1.75 Ga and the Gothian orogeny from 1.75-1-5 Ga (Gaál and Gorbatschev, 1987). Later events, mainly the Sveconorwegian-Grenvillian orogeny and the Caledonian orogeny from 1.14-0.9 (Bingen et al., 2008) and 0.5-0.4, respectively, along with rifting and continental igneous activity led to reworking of the Baltic shield (Gaál and Gorbatschev, 1987).

Fennoscandia is composed of an Archean core and represents the northwestern part of Baltica (Bingen et al., 2008). The Sveconorwegian orogeny resulted from collision between Fennoscandia and a major plate, postulated to be Amazonia (Bingen et al., 2008), and divides into four mainly Mesoproterozoic terranes and a Paleoproterozoic Eastern segment (figure 7).

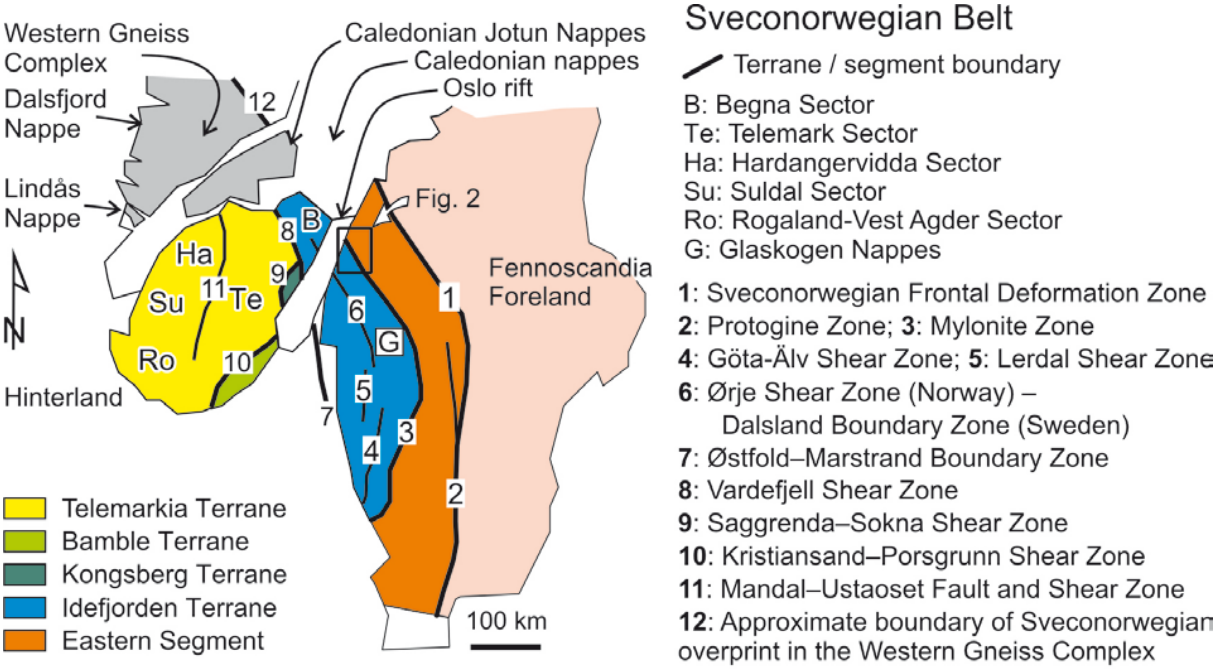

Figure 7. Map of Scandinavia showing the main lithotectonic units. Figure from Bingen et al., 2008.

The Eastern segment is mainly made up of 1800-1640 Ma gneissic granitoids, intruded by 1560 Ma mafic dykes, 1460-1380 Ma granite dykes and plutons and 1250-1200 Ma granite plutons (Bingen et al., 2008). The Idefjorden Terrane consists of 1660-1520 Ma calc-alkaline and tholeiitic plutonic and volcanic rocks, associated with greywacke bearing metasedimentary sequences, overlain by the supracrustal Dal Group. The Bamble and Kongsberg Terranes are made up of 1570-1460 Ma calc-alkaline plutonic suites associated with metasedimentary complexes. The Bamble Terrane consist of the 1200-1180 Ma Tromøy complex, 1170-1150 Ma metaplutons, 1060 Ma pegmatites and 990-920 Ma granite plutons (Bingen et al., 2008). A metamorphic phase affecting both the Bamble and Kongsberg Terranes, yields a monazite age at 1107 ±9 Ma and titanite ages between 1106 ±2 and 1091 ±2 Ma in Bamble, and zircon age at 1102 ±28 Ma and titanite age at 1080 ±3 Ma in the Kongsberg Terrane, reflecting the peak of amphibolite-facies metamorphism caused by collision between the Telemarkia and Idefjorden Terranes (Bingen et al., 2008 and references therein). An earlier metamorphic phase is recognised in the Bamble Terrane by zircon ages at 1125 ±46 Ma and 1124 ±8 Ma and probably dates peak granulite-facies conditions (Bingen et al, 2008 and references therein). The boundary between the Bamble and the Telemarkia Terrane is marked by the Kristiansund-Porsgrunn Shear Zone, in which a late-Sveconorwegian cooling between 910 and 860 Ma is evident (Bingen et al., 2008). The Telemarkia Terrane is characterized by 1520-1480 Ma volcanic and plutonic suites, interlayered and overlain by quartzite-bearing metasedimentary sequences older than ca 1350 Ma and further intruded and unconformably overlain by magmatic suites and sediments between 1280 Ma and 1130 Ma (Bingen et al., 2008). The voluminous Sveconorwegian plutonism has its location in the Telemarkia Terrane. Andersen (2005), however, criticises this nomenclature and division of Terranse in the Sveconorwegian orogeny, arguing that a lack of information renders the Terrane nomenclature in conflict with central concepts of Terrane analysis. The Sveconorwegian orogeny is divided into four orogenic phases by Bingen et al. 2008: 1) The Arendal phase at 1140-1080 Ma by collision of Idefjorden and Telemarkia, generating the Bamble and Kongsberg orogenic wedges, 2) The Agder phase at 1050-980 Ma as a result of continent-continent collision, 3) The Falkenberg phase at 980-970

Ma, representing the last step of foreland propagation, and 4) The Dalane phase representing gravitational collapse (Bingen et al., 2008).

Bingen et al. 2008 gives a review of published, mainly U-Pb, geochronological data recording magmatic and metamorphic events in the Sveconorwegian belt.

2.4 Scandinavian Caledonides

The Sveconorwegian orogeny lasted from 900-600 Ma with rifting of both the Laurentian and Baltican plates and development of Neoproterozoic basins (Gee et al. 2008). The separation of Laurentia and Baltica from Rodinia culminated in the Vendian at ca 600 Ma, with intrusion of mafic dyke swarms (Gee et al., 2008). Black shales were deposited and dominating Baltica and carbonates were dominating Laurentia.

Black shale and carbonate deposition characterize the lower successions of the marginal basins of Baltica and Laurentia, respectively. Most of these subsiding Neoproterozoic basins, however, were filled by thick successions of predominantly coarse clastic sediments.

The marine transgression along the Baltica margin, progressing southwards from the Mjøsa district (Cambrian) to the central Oslo Region (lower Ordovician), is characterized by a basal conglomerate and black shale (alun shale). Further deposition resulted in a 1 km thick marine succession of Ordovician shales and limestones under Silurian limestones. The 1 km thick upper Silurian Ringerike sandstone units represents the Caledonian foreland basin fill which might have reached a maximum pre-erosional thickness of 2-4 km.

The Scandinavian Caledonides started with subduction along the Laurentian side of the Iapetus Ocean during the early Ordovician (Pedersen et al. 1992) and culminated with a major continent-continent collision between the Laurentian and Baltican plates in Silurian to early Devonian time (e.g. Roberts et al., 2003; Gee et al., 2008).

The orogeny can be divided in two phases, an early and a late phase. The early phase is linked to arc – arc and/or arc – continent collision, an event associated with the Taconian/Grampian event. The latter event, termed The Scandian event (ca 430-390 Ma), involved major nappe (thrust sheet) emplacement and rapid subduction and exhumation (Roberts, 2003).

Extensional collapse followed the continent collision, first through ductile and later through brittle deformation (Fossen, 2010). The change from contractional to extensional tectonics happened in the south at about 400 Ma.

Remnants of the Caledonides can be traced from the Stavanger Region in southern Norway and 1500 km northward to the Barents Sea region (Corfu et al., 2014). In the east along the Caledonian front, a thin sedimentary succession of Vendian-Cambrian age lies unconformably upon older Precambrian crystalline basement (rocks of the Fennoscandian shield) (Roberts et al., 2007). The Caledonides disappear below younger Palaeozoic to Cenozoic sedimentary rocks in the west and north.

Distinct tectonostratigraphic units were organized by Roberts and Gee (1985) into Lower, Middle, Upper and Uppermost Allochthons. The Lower and Middle Allochthons have been interpreted to have been derived from Baltica, the Upper Allochthons are considered to be exotic in respect in respect to Baltica representing the Iapetus (Roberts, 2007) and the Uppermost Allochtons are considered to be derived from either Laurentia or unknown microcontinents (Roberts, 2007).

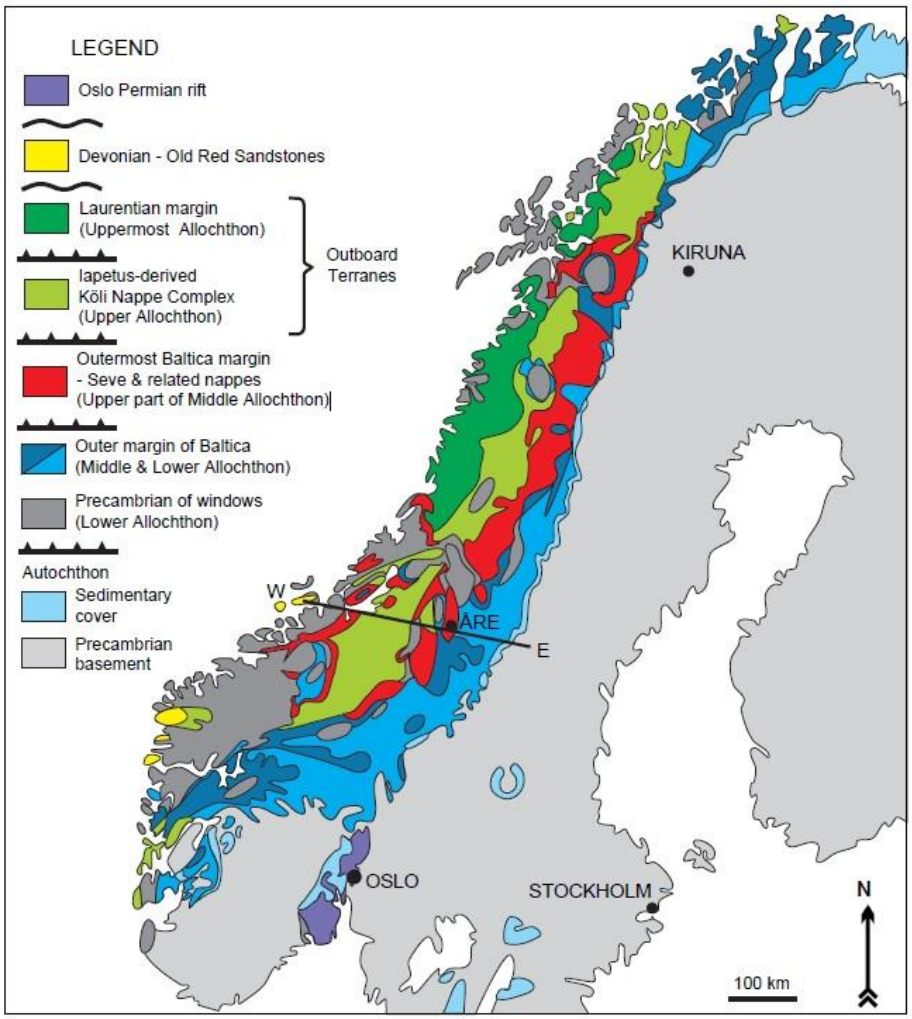

Figure 8. Tectonic map showing the Scandinavian Caledonides. Figure from Gee et al. 2010.

2.5 Oslo region

The Oslo region includes both the Permian rift and the frontal part of a foreland fold and thrust belt (Morley, 1986). The term Oslo Region refers to an area that extends 115 km north and south of the city of Oslo. It is 40 – 70 km in width and covers an area of approximately 10,000 km^2, a province of Paleozoic rocks (e.g. Bruton et al. 2010; Neumann et al., 1992). The Oslo rift is a late Carboniferous to early Permian transtensional and extensional basin, located in Proterozoic crust (Neumann et al. 1992). The Oslo rift (figure 9) is the northern most part of the Rotliegendes basin and comprises three linked up segments in an en-echelon

array, the Rendalen Graben, the Oslo Graben which consist of the two half-grabens Akershus Graben and Vestfold Graben, and the offshore Skagerrak Graben (Larsen et al. 2008). Including the Rendalen Graben, the total length of the Oslo rift is about 500 km. In the Oslo graben, which is exposed on land, Paleozoic sedimentary and magmatic rocks are preserved, whereas Precambrian metamorphic rocks are to be found in areas to the east and west (Neumann et al. 1992). The Precambrian basement rocks are exposed along both rims of the rift (Larsen et al. 2008) with a 2000 m thick succession of Cambro-Silurian limestones, shales and sandstones overlying the basement rocks (Bruton et al. 2010). The Asker Group, a 40 – 120 m thick sequence of continental to shallow marine sedimentary rocks lies unconformably on top of the eroded Cambro-Silurian sedimentary sequence (Neumann et al. 1992). The Palaeozoic succession has been dissected by a series of Upper Palaeozoic lavas, dykes and sills, causing local metamorphism (Bruton et al. 2010).

The formation of the Oslo Graben developed over a period of some 50 million years, from the end of the Carboniferous throughout much of the Permian (e.g. Corfu and Dahlgren, 2008) and is interpreted to be related tectonically to the last phase of the Variscan Orogeny (e.g. Larsen et al., 2008). Two main factors explain the development of the Oslo rift. First, an abnormally high temperature caused a weakening of the crust, then a lithospheric stretching north of the Tornquist fault system (Larsen et al. 2007; Larsen et al. 2008) caused a rift and graben to develop. Torsvik et al. (2007), however, suggests that rifting was caused by a mantle plume. The development and formation of the Oslo Rift has been described in six steps: 1) A proto-rift forerunner to rifting, 2) The initial rift and first basaltic volcanism, 3) The rift climax, with rhomb porphyry fissure volcanoes, 4) The mature rift, with central volcanoes and caldera collapse, 5) A magmatic aftermath, with major batholiths, and 6) Rift termination with small granite intrusions (e.g. Olaussen et al. 1994; Larsen et al. 2008).

The Brunlanes alkalic basalts have been dated to 300.4±0.7 Ma and 299.9±0.9 Ma by perovskite and are among the earliest magmatic products of the Oslo rift. The Larvik batholith consists of 10 plutons and covers an area of about 1000 km^2 (Petersen, 1978). The plutons are roughly circular and repeatedly cut each other in a westward direction. The two oldest plutons in the east are quartz-bearing larvikites, the next six (younger) plutons towards the west are silica saturated or contain minor amounts of nepheline and the two youngest plutons in the northwest of the batholith are nepheline rich (Petersen, 1978; Dahlgren et al., 1996). The

second larvikite pluton has been dated at 298.6±1.4 Ma and the ninth pluton has been dated at 292.1±0.8 Ma (Dahlgren et al., 1996), giving a period of 5-6 years where the entire plutonic complex has been emplaced.

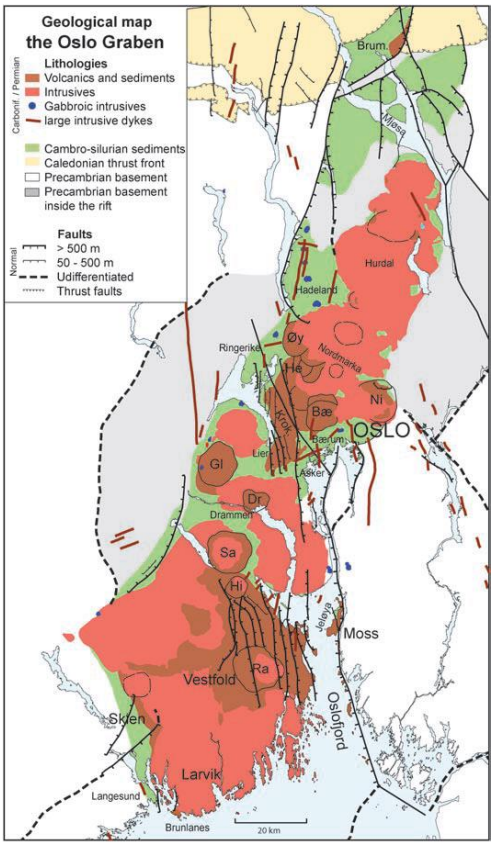

Figure 9. Simple geological map, showing the Oslo Graben. Figure from Larsen et al. 2008.

3. Methods

Zircon is widespread in igneous, metamorphic and sedimentary rocks. With its high closing temperature (i.e. blocking temperature for Pb) of at least 900°C, the zircon will withstand periods of high-grade metamorphism and partial melting of the host rock (Lee, Williams and Ellis, 1997). The refractory nature of zircon facilitates the preservation of a closed isotopic decay system. With sufficient amounts of Pb and U for measurement, little initial Pb and known decay constants, zircon makes a very useful chronometer. The decay of U and Th through intermediate steps to Pb will give rise to predictable amounts of He, alongside with fission tracks by spontaneous fission of ^{238}U, making the zircon a great tool for low-temperature thermochronometry. For the mentioned reasons, zircon is one of the most used minerals in geochronometry, with a wide range of applications.

3.1 U-Pb

There are two naturally occurring and long-lived Uranium isotopes with half-lives of 0.7 Ga (^{235}U) and 4.5 Ga (^{238}U). With a half-live of 14.1 Ga ^{232}Th is the only naturally occurring long-lived isotope of thorium. In addition, there are several short-lived isotopes of U and Th, and the decay chains from ^{238}U, ^{235}U and ^{232}Th include five Th-isotopes and one U-isotope. The isotopes ^{238}U, ^{235}U and ^{232}Th decay through a series of intermediate daughter products to ^{206}Pb, ^{207}Pb and ^{208}Pb, respectively, as summarized in the following equations:

1) $^{238}U \rightarrow {}^{206}Pb + 8{}^{4}He + 6\beta^{-} + Q$
2) $^{235}U \rightarrow {}^{207}Pb + 7{}^{4}He + 4\beta^{-} + Q$
3) $^{232}Th \rightarrow {}^{208}Pb + 6{}^{4}He + 4\beta^{-} + Q$

In these decay expressions, Q, β^{-} and ^{4}He represents the sum of decay energies of the entire series and the emitted β^{-} and alpha-particles, respectively. The chains are branched, but lead is the stable end product of all possible paths. The half-lives of ^{238}U, ^{235}U and ^{232}Th (summarized in table 1) are much longer than the intermediate daughter products.

Table 1. Abundances, half-lives and decay constants of naturally occurring isotopes of U and Th

Isotope	Abundance (%)	Half-life (years)	Decay Constant (y^{-1})
^{238}U	99.2743	4.468×10^{9}	1.55125×10^{-10}
^{235}U	0.7200	0.7038×10^{9}	9.8485×10^{-10}
^{232}Th	100	$14.010. \times 10^{9}$	4.9475×10^{-11}

Reference: Steiger and Jäger, 1977, Faure and Mensing, 2005.

The decay will therefore, eventually, reach secular equilibrium, a steady state where the decay rates of the intermediate daughters are equal to their rate of formation. The intermediate daughters can then be disregarded and we can derive a complete description of the number of radiogenic atoms D by equation 4, where D_0 is the initial number of daughter atoms, N is the total number of the parent atom, λ is the decay constant and t is the time:

$$4) \quad D = D_0 + N(e^{\lambda t} - 1)$$

Although ^{204}Pb in principle is radioactive, its half-life is so long (1.4×10^{17} y) that it can be regarded as a stable (or nonradioactive) isotope. Mass spectrometers are suitable for measuring isotope ratios, rather than absolute abundances. Therefore, equation 4 can be divided by ^{204}Pb to give three equations for age determination by decay of U and Th to Pb, where the subscript *i* refer to the initial values, *λ1, λ2, and λ3* to the decay constants and t to the time:

$$5) \quad \frac{206Pb}{204Pb} = \left(\frac{206Pb}{204Pb}\right)_i + \frac{238U}{204Pb}\left(e^{\lambda 1 t} - 1\right)$$

$$6)\ \frac{207Pb}{204Pb} = \left(\frac{207Pb}{204Pb}\right)_i + \frac{235U}{204Pb}\left(e^{\lambda 2t} - 1\right)$$

$$7)\ \frac{208Pb}{204Pb} = \left(\frac{208Pb}{204Pb}\right)_i + \frac{232Th}{204Pb}\left(e^{\lambda 3t} - 1\right)$$

U and Th are both High Field Strength Element (HFSE), substituting as U^{4+} and Th^{4+}, respectively, with Zr^{4+} in the crystal structure of zircon. Lead is, however, considered a Large Ion Lithophile Element (LILE) in silicate systems, forming Pb^{2+}, and in contrast to U^{4+} and Th^{4+} which have a similar radii as Zr^{4+}, Pb will usually not fit in the crystal structure. The time t in equation 4 – 7 therefore represents the time of crystallization when U and Th is included in the crystal structure while Pb is excluded. Lead is also a more mobile element than U and Th, except in oxidizing environments, and although zircon is quite resistant with a high blocking temperature (as noted above), some lead loss might occur from zircon in metamorphic and hydrothermal events. The emission of α-particles, and related nuclear recoil, causes radiation damage in crystals, and will also contribute to the loss of Pb and other intermediate daughters. By plotting the two parallel U decay series against each other in a Concordia diagram, the loss or gain of U, Th or Pb can be represented by a graphical procedure. Given the two different half-lives of the U decay systems and no loss or gain of U, Th or Pb, all ages will fall on the Concordia curve. Since the Pb isotopes will not fractionate, simple Pb-loss will cause a systematic downward deviation from the curve (in the direction towards zero on both axes); the ages will be discordant. Discordant ages can also result from mixing of components with different ages in different parts of the zircon e.g. older or younger core than the rim.

3.2 U-He

The three decay series given in equation 1 – 3 produce 8, 7 and 6 α-particles (^{4}He), respectively, for each radioactive parent atom. The total number of radiogenic ^{4}He for the three series in combination is expressed in equation 8, where the subscript N signifies the numbers of atoms per gram of sample and λ the decay constants:

$$8)\ \left(^4He\right)_N = 8\left(^{238}U\right)_N\left(e^{\lambda 1t} - 1\right) + 7\left(^{235}U\right)_N\left(e^{\lambda 2t} - 1\right) + 6\left(^{232}Th\right)_N\left(e^{\lambda 3t} - 1\right)$$

Negligible amounts of ^{4}He are generated by the decay of ^{147}Sm, and are ignored. Equation 8 assumes that there is no non-radiogenic ^{4}He present in the crystal.

He will be lost by thermally activated volume diffusion, following linear Arrhenius relationship and given in equation 9. D is the diffusivity, D_0/a^2 is the frequency factor, "a" is the diffusion domain radius, E_A is the activation energy, R is the gas constant and T is the temperature in Kelvin:

$$9) \quad \frac{D}{a^2} = \frac{D_0}{a^2} e^{-E_A/RT}$$

Diffusion is driven by the He concentration gradient in the crystal, as shown by Fick`s first law:

$$10) \; F = -D \frac{\partial C}{\partial X}$$

where F denotes the mass flux, D the diffusivity and $\partial C/\partial X$ is the concentration gradient. The description of change in concentration with time as a function of the concentration gradient is given by Fick`s second law. Equation 11 assumes spherical geometries, where r is the radius of the sphere and t is the time:

$$11) \; \frac{\partial C}{\partial t} = D \left(\frac{\partial^2 C}{\partial r^2} + \frac{2}{r} \frac{\partial C}{\partial r} \right)$$

Departure from linearity in early stages of Arrhenius has been shown, and is discussed later in the text.

He will be lost by ejection of α-particles, depending on the parent nuclides distance from the crystal surface and the alpha particles trajectory. This may cause an underestimation of the true age and needs to be corrected for. The correction is dependent on the size and geometry of the crystal (Farley et al. 1996) as well as the zonation of the crystal and related distribution of U and Th (e.g. Dobson et al. 2008). The Ft was calculated following Farley et al. 1996, and by dividing the measured age by Ft will you get the corrected age. The stopping distance for

alpha particles, although dependent on their kinetic energy, reaches about 20 μm (Farley et al., 1996).

3.3 Sample preparation and ID-TIMS (Isotope Dilution Thermal Ionization Mass Spectrometry) analysis of U-Th-Pb

As Precambrian xenocrystic zircon grains would be a "smoking gun" to confirm the crustal contamination hypothesis (see introduction), extra care is needed to reduce the risk of contamination. Sampling in river sediments has several advantages:

a) River samples represent erosional products in a wide up-stream drainage area where heavier minerals tend to concentrate, increasing the efficiency of the sampling.
b) By sampling river sediments with a pan the need for crushing operations and usage of Wilfley table is eliminated, reducing the risk of contamination.
c) On site, heavy mineral washing will reduce the sample sizes, making the sampling process more efficient and practical.

After sampling and pre-concentration of the heavy minerals, the samples were sealed in small plastic bags until further laboratory work at the University of Oslo.

All the equipment for separation was disassembled and washed in an ultrasonic bath for 15 min. and then air blown. The samples were washed with alcohol, dried at 50°C for approximately 24 hours and sieved at 250μm. Further mineral separation involved a Frantz magnetic separator, heavy liquid (methylene iodide) and hand picking in alcohol under a binocular microscope. The most promising zircons, the ones that looked the "oldest" were then selected. The main selection criteria were sub- to anhedral grains, colored and inclusion-rich grains and/or grains with a possible older core. However, most of the zircons were euhedral and transparent with only a few having a distinct core. Since the xenocrystic zircon grains in question (as explained in the introduction) are quite old compared to the igneous zircons with an age of 3.5 – 18.4 ka (Bindeman et al., 2011), no abrasion was needed. The selected grains were washed with HNO_3, H_2O and acetone and weighed on a micro-balance, before the zircons and a $^{202}Pb/^{205}Pb$ / ^{235}U spike of known concentration were put in Teflon bombs for dissolution with HF + HNO_3 at 195°C for 5 days (Krogh 1973). The bombs were

then removed from the oven and the acid solutions were evaporated on a hotplate. Ten drops of 3 N HCl were added before the bombs were put back in the oven for one more day.

The samples were evaporated on a hotplate and loaded with H_3PO_4 and Si gel on a Re-filament before measuring in a MAT262 mass spectrometer in static mode with Faraday cups, or peak jumping in a secondary electron multiplier (SEM) for the weaker signals. Fractionation was corrected for 0.1 %/amu for Pb and 0.12%/amu for U, but for those measured in static mode, using Faraday cups, the fractionation factor was determined directly from the obtained $^{205}Pb/^{202}Pb$ ratio (known in the spike). The model of Stacey and Kramers, (1975) was used to correct for any initial Pb beyond the 2 pg Pb (and 0.1 pg U) assumed to be, and corrected as blank. A standard solution, NBS 982 mixed with U-500, was used to check for reproducibility and proper functioning of the instrument. The decay constants are taken from Jaffey et al. (1971) and for the modern day U composition we used $^{238}U/^{235}U$ = 137.88. One of the measured zircons is excluded from the data set because of nonsensical ages, giving; 207/206- age of 0.0 Ma, 207/235- age of 539.8 Ma and 206/238-age of 901.7 Ma.

3.4 Sample preparation and – combined (U-Th)/He and U-Pb analysis

For the second part of the thesis, zircons were picked in alcohol under a binocular microscope from seven samples from south and south east of Norway, previously separated by other students and/or researchers, at the University of Oslo. Zircons with a euhedral shape and lacking inclusions were then capsulated in 99.9% pure Pt-tubes for further laboratory work at SUERC. Five zircons from the sample 743-03 (from a larvikite) had previously been air-abraded. At SUERC, the Pt-tubes were placed in a Cu planchet along with three standards (Fish Canyon Tuff – FCT). However, one of the FCT zircon grains was lost, presumably during loading into the Pt-tubes, while the He was lost for one of the other two zircons during measurement. Therefore, only one measurement for FCT was acquired; however, the age is inconsistent with previously measured and calculated ages for FCT (see discussion; e.g. Foeken et al., 2006).

3.4.1 Diode laser heating and He measurement

Two pumps, turbo-molecular and triode ion- pump in combination (figure 1); bring the system to UHV conditions (< 10^{-9} torr). The Pt-tubes were heated for 15 – 20 min. with an 808 nm diode laser at temperatures ranging from 1100°C to 1300°C, and then reheated under the same conditions and length of time to ensure complete He extraction. The temperatures of the Pt-tubes are measured indirectly, by visual observation of the color emitted from the heated capsules. The gas liberated from the Pt-tubes was then purified using a hot SAES TiZr getter and two charcoal traps cooled by liquid nitrogen. The abundances of He were measured by an electron multiplier in a Hiden HAL3F quadrupole mass spectrometer operated in static mode. Absolute He concentrations were calculated by comparing peak height with a calibrated standard. Cold blank was measured routinely to correct for any drift in measured background He abundances throughout the day. Hot blank was measured to correct for any atmospheric He possibly stuck to the Cu planchet or Pt-tubes. See Foeken et al., (2006) for detailed analytical procedure.

Further analysis of the zircons was performed at the University of Oslo after removing the grains from the Pt-tubes. This analytical stage followed the same procedure of dissolution and measurement (ID-TIMS) as stated above. Five zircons weighing more than a few micrograms, however, were passed through an ion exchange resin using HCl solutions (Krogh 1973; Corfu 2004).

All Concordia diagrams were plotted using Isoplot 4.

4. Results

4.1 Samples and sample localities

The search for additional Precambrian xenocrystic zircon grains in Iceland was started during the summer of 2013. Fourteen sediment samples were taken from rather small rivers across the Öræfajökull area, shown in figure 10. After mineral separation, twelve zircons were selected from six of the samples for further investigation; however, one of the zircons gave results similar to previously measured blanks, and is excluded from the dataset. A brief description of the sample localities and zircon morphology, based on binocular microscope images, follows below. All of the samples have high abundances of euhedral and transparent zircons rather small in size (50–300 μm). Two smaller samples from Vattará and west of Reynivellir are almost devoid of zircons.

Figure 20. Map over Öræfajökull, showing sample localities: 1, DAV-13-1; 4, DAV-13-4; 6, DAV-13-6; 8, DAV-13-8; 11, DAV-13-11; 14, DAV-13-14.

Broadly matching U/Pb and U+Th/He ages of Proterozoic zircons extracted from sediment and hyaloclastite samples from the Öræfajökull area (Corfu, unpublished data), motivated a supplementary investigation of U/Pb and U+Th/He zircon ages of different lithologies and tectono-thermal environments in southern Norway.

The U-Pb ages are given in table 2 and 3, whereas a short description of the localities and Concordia ages (figure 17-23) are given in the subsequent text. The incomplete information for some of the data in table 2, 3 and 4 (SB1, GB1, HVRT1, SAL 679, 743-03, S2 and BR) is a result of lack of information from the previous datasets.

He ages are given in table 4 with U-Pb ages for the same samples for easy comparison. Alpha ejection corrections are done following Farley et al. (1996); however, a greater uncertainty than given in table 4 arises from the fact that the length and width of the small zircons were measured with a ruler and that alpha ejection correction have the greatest effect for small crystals. Alpha ejection corrections were performed for the zircons dated by F. Stuart at SUERC (SAL 679, SB1, GB1, HVRT1) prior to this study. Correction for zircon zonation has not been performed, and the corrected ages should therefore be seen as approximations in an effort to address the problems stated earlier (see introduction). Due to time constraints, most samples only have a single or a few new measurements.

4.1.1 DAV-13-1 383/8 (63°54.670/16°36.835)

The sample DAV-13-1 383/8 was collected at about 700 m a.s.l. in order to address the possibility of zircon contamination of sedimentary units by ice-rafted sand and gravel, e.g. from east Greenland. The Holocene upper marine limit has been found to occur at 150 m a.s.l. (Norddahl, et al. 2008), well below the sample site. The sample was taken from sediments next to glacier deposits (i.e. sand deposited from melt water[?]),

Figure 11. Image of DAV-13-1 383/8. The length is approximately 260 μm.

about 300 m above a radiostation near Hnappavellir, SW of Kviarjökull. The sample contained several euhedral zircons with overgrowths, and a few transparent and euhedral zircons had grown together. A small fraction of the zircons, ca 10 – 20 % were to some degree rounded (subhedral). The selected zircon had some minor overgrowth (see figure 11) and a distinct darker and grey looking core [showing mottled texture]. The U-Pb age reveals a young igneous zircon. The sample HVRT1 dated in 2013 by F.Corfu was collected from a small stream on the plain below the radiostation at Hnappavellir. The 2013 dating yielded one zircon of zero-age and one Precambrian zircon at 789.1 ±7.6 Ma ($^{206}Pb/^{238}U$), 856.2 ±34.9 Ma ($^{207}Pb/^{235}U$) and 1033 ±114.4 Ma ($^{207}Pb/^{206}Pb$). The Precambrian zircon had an overlapping He-age at 916.0 Ma

4.1.2 DAV-13-4 383/9 and 383/10 (64°08.085/16°05.899)

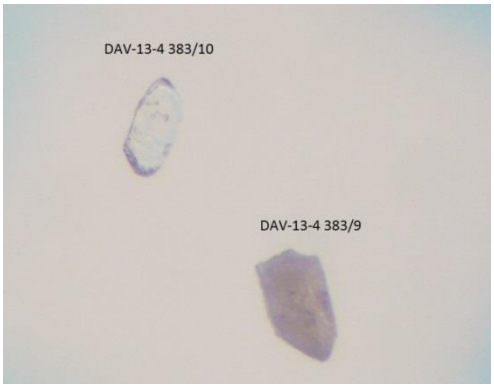

Figure 12. Binocular picture of: DAV-13-4 383/9, 190 μm; DAV-13-4 383/10, 160 μm.

The sample DAV-13-4 was collected from dry sediments, west of Reynivellir at the bottom of a small waterfall in the river Fjallsá. The sample contained 5 metamict and euhedral to subhedral zircons with broken of tips and several subhedral and transparent zircons with minor inclusions (see figure 12). The subhedral zircon, DAV-13-4 383/10, gives young U-Pb ages of 1.8 ±0.2 Ma ($^{206}Pb/^{238}U$) and -0.9 ±1.9 Ma ($^{207}Pb/^{235}U$), whereas DAV-13-4 383/9 is dated at 30.8 ±3 Ma ($^{206}Pb/^{238}U$), 49.3 ±32.4 Ma ($^{207}Pb/^{235}U$) and 1081 ±951.3 Ma ($^{207}Pb/^{206}Pb$), predating the oldest rocks in Iceland (see discussion).

4.1.3 DAV-13-6 383/1, 383/2 and 383/3 (64°04.364/16°20.968)

The sample DAV-13-6 was collected from sediments in the river formed by melt water from the glacier

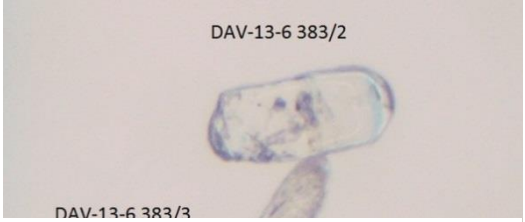

Figure 13. Image of: DAV-13-6 383/1, 130 μm; DAV-13-6 383/2, 230 μm; DAV-13-3 383/3, 150 μm.

Breidamerkurjökull between Breidarlón and Jokulsarlón. This sample contained the highest amount of zircons with a morphology that differs from the high amount of euhedral, transparent and intact igneous zircons seen in all but two of the samples. Three of the zircons that seemed to differ the most and fulfilling the criteria for selection (see method) are seen in figure 13. The euhedral to subhedral zircon DAV-13-6 383/1 is somewhat fractured with the one end partly missing and a darker more grey area at the other end. Two small inclusions are barely visible in figure 13, but more easily seen under a binocular microscope. The U-Pb ages for this zircon are 5.1 ±0.1 Ma ($^{206}Pb/^{238}U$) and 4.8 ±1.4 Ma ($^{207}Pb/^{235}U$), predating igneous zircons in the Öræfajökull area, ranging from 3.5 ka to 34.3 ka (Bindeman et al., 2011). The largest zircon, DAV-13-6 383/2, is clearly rounded, with some minor cracks and inclusions, yielding U-Pb ages of 1.2 ±0.1 Ma ($^{206}Pb/^{238}U$) and 0.7 ±1.2 Ma ($^{207}Pb/^{235}U$). The zircon DAV-13-6 383/3 is partly rounded with some minor cracks and yields U-Pb ages of 8.9 ±0.5 Ma ($^{206}Pb/^{238}U$) and 7.7 ±7.4 Ma ($^{207}Pb/^{235}U$), also predating previously reported igneous zircons from the Öræfajökull area.

4.1.4 DAV-13-8 383/4: (63°59.867/16°23.950)

The sample DAV-13-8 was collected in a small river called Hruta nearby Fjallsjökull, some hundred meters from the road, revealing only a few zircons differing in morphology from the euhedral and transparent igneous zircons. The zircon DAV-13-8 383/4 is subhedral to anhedral, is somewhat cracked, has a clearly visible inclusion (orange in figure 14) and gives U-Pb ages of 1.1±0.3 Ma ($^{206}Pb/^{238}U$) and -1.6 ±1.7 Ma ($^{207}Pb/^{235}U$).

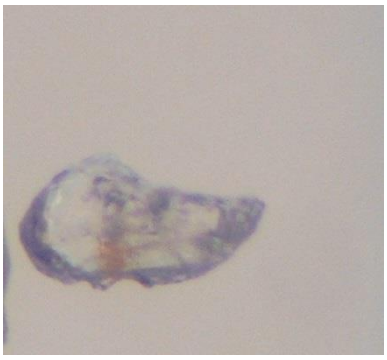

Figure 14. Image of DAV-13-8 383/4, 260 μm.

4.1.5 DAV-13-11 383/5 and 383/11 (63°55.122/16°34.513)

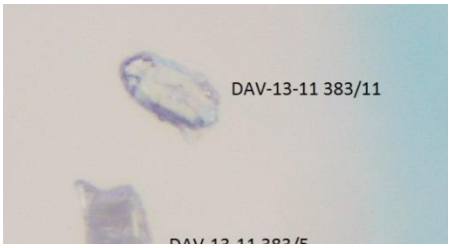

Figure 15. Image of DAV-13-11 383/5, 130 μm; DAV-13-11 383/11, 140 μm.

The sample DAV-13-11 was collected at about 0.5-1 km away from Stigá Bridge towards the inland, in the river Stigá that seemed to form from a water fall farther up in the mountains. The sample contained mostly the previously mentioned euhedral igneous zircons, but also a few of the zircons with a mottled grey interior (see figure 15). The zircon DAV-13-11 385/5 gave ages of 0.7 ±0.5 Ma ($^{206}Pb/^{238}U$) and 5.5 ±5.6 Ma ($^{207}Pb/^{235}U$), whereas the more transparent and rounded zircon, DAV-13-11 383/11 gave U-Pb ages of 3.5 ±1.8 Ma ($^{206}Pb/^{238}U$) and -6.3 ±34.7 Ma ($^{207}Pb/^{235}U$). The samples SB1 377/19, SB1 377/20 and SB1 377/21, gathered by R.G.Trønnes in 2003, stems from the same river. The zircons are essentially of zero-age (within the margin of error).

4.1.6 DAV-13-14 383/6 and 383/7 (63°54.698/16°43.610)

The sample DAV-13-14 was collected about 200-300 m away from the road at Hvalördugilslækur at a small river disappearing into the ground. The sample contained a few zircons with grey interior and some overgrowth, and a few light orange and yellow euhedral zircons (see figure 16). Both the zircons gave U-Pb ages of zero (within the margin of error).

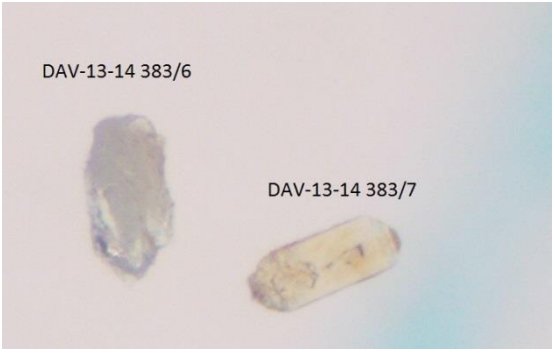

Figure 16. Image of DAV-13-14 383/6, 200 μm; DAV-13-14 383/7, 180 μm.

4.1.7 GB1

The sample GB1 was collected at a river called Gljúfúrsá River by R.G.Trønnes in 2003. One of the zircons (GB1 377/22) gave a U-Pb age of zero; however, the zircon had an inconsistent U-He age of 99.0 Ma. The sample was measured for He by Fin Stuart, at a time when there supposedly could have been a problem with measuring cold blank, potentially explaining this inconsistency. The zircon GB1 377/23 gave U-Pb ages of 947.6 ±2.0 Ma ($^{206}Pb/^{238}U$), 1148.9 ±2.2 Ma ($^{207}Pb/^{235}U$) and 1551.7 ±2.7 Ma ($^{207}Pb/^{206}Pb$), and a similar U-He-age of 1250.0 Ma.

The zircon GB1 377/24 gave U-Pb ages of 848.7 ±2.0 Ma ($^{206}Pb/^{238}U$), 1041.9 ±2.0 Ma ($^{207}Pb/^{235}U$) and 1473.0 ±2.7 Ma ($^{207}Pb/^{206}Pb$), and a similar U-He age of 1070.0 Ma.

4.1.8 SAL 779

The sample SAL 779 stems from a thin basalt flow within a hyaloclastite unit. Two zircons were measured in 2013 by F.Corfu, giving one of the zircon U-Pb ages of 37.0 Ma ($^{206}Pb/^{238}U$) and 38.8 Ma ($^{207}Pb/^{235}U$), and one Precambrian zircon at 690.8 ±1.4 Ma ($^{206}Pb/^{238}U$) and 832.7 ±1.9 Ma ($^{207}Pb/^{235}U$) and 1233 ±4.2 Ma ($^{207}Pb/^{206}Pb$). The Cenozoic zircon gave an U-He age of 9.4 Ma, while the Precambrian zircon gave a similar U-He age of 1132 Ma.

4.1.9 743-03 - Larvik

The zircons 743-03-1 to 743-03-5 are new and added to previously unpublished data from F.Corfu and S.Dahlgren (1996) from a larvikite in Larvik. Figure 19a shows all but one Concordia point, giving a lower intercept age of 276 Ma and an upper intercept at 316 Ma, with large errors due to clustering of the data points near the Concordia curve. The filled error ellipses represents the old data, clustering around 294 Ma, whereas the open ellipses are the new data with a higher scatter of points ranging from just below 290 to above 296 Ma, representing the formation of the larvikite plutonic complex. Adding all new points in figure 19b, the upper intercept gives an age of 289.1 Ma, due to the extra highly discordant (-27.5%) data point (743-03-4). The discordant data point gave ages of 366.4 ±1.9 Ma ($^{206}Pb/^{238}U$) and 356.1 ±2.1 Ma ($^{207}Pb/^{235}U$). The U-He ages for the selected zircons are ranging from 326.66 Ma to 597.77 Ma, well above the age of formation. The early Permian larvikites have undergone insignificant deformation and alteration and are generally characterized by relatively high Zr-content and well crystallized and inclusion-poor zircon grains. The inconsistency may therefore arise from incomplete dissolution of the larvikite zircons before ID-TIMS at the University of Oslo. The helium extraction at SUERC might have annealed the already abraded zircons and made the zircons refractory enough to withstand the dissolution process, potentially also explaining the highly discordant data point (743-03-4).

4.1.10 S2 - Gjersjøen

The sample S2 was collected from an augen gneiss in Kolbotn next to Gjersjøen and dated in 2000 by A.Zahid for a master thesis. Kolbotn is situated outside the Oslo rift, about 12 km SSE of the city of Oslo, and is located in the Idefjorden Terrane Complete rock and location description, along with data for S2/ZIR1 and S2/ZIR5 are given in Zahid (2000). Of the two zircons measured for this thesis, S2-2 and S2-3, only the latter was measured for He extraction, giving an U-He age of 301.02 ± 44.53 Ma (see table 4). The S2-2 shows slightly older U-Pb ages compared to the previous data from Zahid, yielding ages of 1401.4 ±4.5 Ma ($^{206}Pb/^{238}U$) and 1442.8 ±3.6 Ma ($^{207}Pb/^{235}U$), whereas S2-3 is consistent with ages of 1356.9 ±3.3 Ma ($^{206}Pb/^{238}U$) and 1377.2 ±2.3 Ma ($^{207}Pb/^{235}U$). The Concordia diagram is given in figure 18 and yields dramatically different ages if plotted only with the old data, giving ages of 869 Ma at the lower intercept and 1512 Ma at the upper intercept. This is in contrast to the age achieved by plotting all data or just the new data (1320 Ma at the lower intercept and 2350 Ma at the upper intercept). The filled error ellipses represent the old Concordia points, whereas the open ellipses are the newly added points. The inconsistent U-Pb age for S2-2 might be a result from an inherited core, giving an older age.

4.1.11 C-06-3 - Nevlunghavn

The sample C-06-3 was collected from an orthogneiss in Nevlunghavn enclosed in larvikite, about 10-15 km SW of the city of Larvik (F.Corfu, unpublished). The three previously dated zircons, C-06-3 172/4, 172/5 and 172/6 were abraided. The zircon C-06-3-1 gave a lower U-Pb age than the zircons previously measured, at 1035.9 ±2.1 Ma ($^{206}Pb/^{238}U$) and 1177.4 ±2.4 Ma ($^{207}Pb/^{235}U$), possibly because of a lack of abrasion. However, C-06-3 gave U-Pb ages of 1367.6 ±5.7 Ma ($^{206}Pb/^{238}U$) and 1432.4 ±4.0 Ma ($^{207}Pb/^{235}U$), in good agreement with previously results (table 3). The Concordia diagram is given in figure Q, showing a lower interception at 302 ±41 Ma, in close correspondence with the emplacement of the larvikite plutonic complex, and an upper interception at 1552.4 ±6.0 Ma. The black squares represent the old data points, whereas the open ellipses represent the new measurements. The U-He ages are 284.45 Ma (C-06-3-1) and 398.43 Ma (C-06-3-3), when corrected for alpha ejection.

4.1.12 STANG4 - Stangnes

The sample STANG4 was sampled in 2007 from a granodioritic gneiss in Stangnes, Kragerø (within the Bamble terrane). Three zircons were during this project in 2014: STANG2, STANG3 and STANG4, giving U-Pb ages ranging from 1224.0 Ma ($^{206}Pb/^{238}U$) and 1246.4 Ma ($^{207}Pb/^{235}U$) to 1497.5 Ma ($^{206}Pb/^{238}U$) and 1511.1 Ma ($^{207}Pb/^{235}U$). The lowermost intercept on the Concordia curve (fig 21) yields an age of 1083.19 ±19 Ma, thought to reflect the peak amphibolite-facies metamorphism in the Bamble terrane, and upper intercept at 1584.8 ±9.6 Ma, reflecting the age of formation of the Zircon. STANG4-3 and STANG4-4, the only two of the three zircons being measured for helium in SUERC, yields U-He ages of 680.79 ±2.42 Ma and 1189.27 ±264.62 Ma, respectively.

4.1.13 C-08-4 - Finse

The sample C-08-4 was collected from a granite in Finse by E. Jensen for a master thesis in 2012. The new zircon added to the dataset from Jensen, E. (2012), C-08-4-3, gives an age of 1087.7 ±5.5 Ma ($^{206}Pb/^{238}U$) and 1114.1 ±4.5 Ma ($^{207}Pb/^{235}U$). This is about 150 Ma older than the E. Jensens oldest age, possibly caused by an older core in the zircon. The Concordia diagram is shown in figure 22, giving a lower intercept at 640 ±540 Ma and an upper intercept at 1102 ±140 Ma with a MSWD of 383. Plotting without the new data, the lower intercept on the concordia curve gives an age of 368 ±26 Ma and upper intercept at 986.7 ±1.9 Ma with a MSWD of 0.38. The lower intercept on the Concordia is probably related to lead loss during the Caledonian Orogeny.

4.1.14 CR-08-7 - Kvitenut

The sample CR-08-7 (figure 23), collected from augen gneiss in the Kvitenut Nappe in an area around Stavsnuten at Hardangervidda, is reported in Roffeis et al. (2013). The U-Pb ages ranges from 1263.4 Ma ($^{206}Pb/^{238}U$) and 1306.3 Ma ($^{207}Pb/^{235}U$) to 1419.7 Ma ($^{206}Pb/^{238}U$) and 1453.9 Ma ($^{207}Pb/^{235}U$), in good agreement with the newly added point (CR-08-7-2) at 1389.9 ±6.3 Ma ($^{206}Pb/^{238}U$) and 1432.8 ±6.4 Ma ($^{207}Pb/^{235}U$). The Concordia diagram, given

in fig. N, gives a lower intercept at 990 ±72 Ma, indicating resetting from the Sveconorwegian Orogeny (Roffeis et al., 2013) and an upper intercept at 1627 ±48 Ma..

4.1.15 BR. – Brunkeberg

The sample BR. is reported in Lajooki et al. (2002) as sample 903 KL-N and 22.1 KL-N from a Brunkeberg formation porphyry in Telemark. The zircons BR.-1, BR.-2 and BR.-3 are the new zircons added to the data set, whereas Br.4 – Br.13 are from Lajooki et al. (2002). The U-Pb ages obtained for the three new zircons are consistent, ranging from 1027.8 ±7.7 Ma ($^{206}Pb/^{238}U$) and 1067.6 ±27.6 Ma ($^{207}Pb/^{235}U$) to 1128.2 ±2.9 Ma ($^{206}Pb/^{238}U$) and 1136.3 ±2.4 Ma ($^{207}Pb/^{235}U$). The Concordia curve is given in figure 17, where the filled error ellipses represent the old points and the open ellipses represent the new data points. Plotting the old data points give a lower intercept age of 1148 ±19 Ma and an upper intercept age of 1509 ±490 Ma. This inconsistent with previously reported upper age at 1155.5 Ma (Lajooki et al. 2002). By plotting only the Concordia curve for the new zircons, a consistent upper intercept at 1153 Ma is achieved, representing the time of crystallization of the Brunkeberg unit. However, the lower intercept at 110 Ma is inconsistent with a reported lower intercept at 400 Ma (Lajooki et al., 2002). The U-He ages for BR.-1 and BR.-2 are 504.73 ±1.6 and 414.47 ±1.4 Ma, respectively.

Table 2. ID-TIMS U-Pb data

					Isotope ratios								Ages (Ma)						
No.	**Weight**	**U**	**Th/U**	**Pbc.**	**^{206}Pb/**	**^{207}Pb/**	**2 σ**	**^{206}Pb/**	**2 σ**	**^{207}Pb/**	**2 σ**	**Rho**	**^{206}Pb/**	**2 σ**	**^{207}Pb/**	**2 σ**	**^{207}Pb/**	**2 σ**	**Disc.**
	(ug)	(ppm)		(pg)	**^{204}Pb**	**^{235}U**		**^{238}U**		**^{206}Pb**			**^{238}U**		**^{235}U**		**^{206}Pb**		
DAV-13-1 383/8	5	893.1	13.0	38.59	18.53	-0.0022	-0.003	-0.00002	0.00005	0.872	1.29824	0.9	-0.1	0.3	-2.3	3.1	0	na	na
DAV-13-4 383/9	2	2783	2.8	26.93	22.27	-0.0009	-0.0018	0.00028	0.00003	-0.024	-0.04755	0	1.8	0.2	-0.9	1.9	0	na	na
DAV-13-4 383/10	1	115.3	1.5	10.14	22.02	0.0498	0.034	0.00478	0.00047	0.075	0.04979	0.3	30.8	3	49.3	32.4	1081	951.3	97.38
DAV-13-6 383/1	1	1576	1.6	5.57	32.69	0.0047	0.0014	0.0008	0.00002	0.043	0.01197	0.4	5.1	0.1	4.8	1.4	0	na	1.3
DAV-13-6 383/2	11	56.9	-1.5	0.84	27.2	0.0007	0.0012	0.00019	0.00001	0.025	0.04585	0.3	1.2	0.1	0.7	1.2	0	na	1.3
DAV-13-6 383/3	1	265.9	1.4	4.85	23.25	0.0076	0.0074	0.00138	0.00008	0.04	0.03844	0.3	8.9	0.5	7.7	7.4	0	na	0
DAV-13-8 383/4	9	104.8	3.7	9.05	18.46	-0.0016	-0.0036	0.00017	0.00005	-0.067	-0.15625	-0.9	1.1	0.3	-1.6	3.7	0	na	na
DAV-13-11 383/5	1	982.8	24.3	12.85	19.16	-0.0055	-0.0053	0.00011	0.00007	-0.357	-0.63996	-1.5	0.7	0.5	-5.6	5.5	0	na	na
DAV-13-11 383/11	1	51.5	3.2	2.39	19.09	-0.0062	-0.0334	0.00054	0.00027	-0.083	-0.72055	-8.5	3.5	1.8	-6.3	34.7	0	na	na
DAV-13-14 383/6	1	1448	4.6	36.67	18.37	-0.0056	-0.0096	-0.00012	-0.00015	0.338	0.58369	0.3	-0.8	1	-5.8	9.9	3652	na	na
DAV-13-14 383/7	1	932.4	-12.4	3.89	18.84	-0.0005	-0.002	0.00002	0.00002	-0.157	-1.21965	-6.1	0.2	0.1	-0.5	2	0	na	na
SAL779 377/13	1	812	0.4	4.4	1317.9	1.2708	0.0042	0.11311	0.00025	0.081	0.00018	0.8	690.8	1.4	832.7	1.9	1233	4.2	46.3
SAL779 377/15	1	45	0.5	3.8	22.0	0.0389	0.0410	0.00576	0.00056	0.049	0.05045	0.3	37.0	3.7	38.8	39.4	na	na	na
HVRT1 377/16	1	1699	--	1.6	20.3	0.0002	0.0008	0.00003	0.00001	0.038	0.20783	0	0.19	0.04	0.2	0.8	na	na	na
HVRT1 377/17	1	28	0.9	6.0	55.6	1.3238	0.0807	0.13029	0.00130	0.074	0.00433	0.3	789.5	7.6	856.2	34.9	1033	114.4	25.0
SB1 377/19	1	5558	--	1.1	19.5	-0.0002	-0.0002	0.00000	0.00000	-0.300	-0.59368	0	0.0	0.0	-0.2	0.2	na	na	na
SB1 377/20	1	67	--	1.0	18.4	-0.0028	-0.0118	0.00004	0.00009	-0.566	-2.71142	0.1	0.2	0.6	-2.8	12.1	na	na	na
SB1 377/21	1	305	--	1.0	18.5	-0.0026	-0.0026	0.00001	0.00002	-1.753	-6.00631	0	0.1	0.1	-2.6	2.7	na	na	na
GB1 377/22	1	300	--	1.9	17.1	-0.0204	-0.0064	-0.00013	-0.00006	1.168	0.24207	0.9	-0.8	0.4	-20.9	6.6	na	na	na
GB1 377/23	1	415	0.3	1.7	2450.5	2.1004	0.0067	0.15836	0.00036	0.096	0.00018	0.8	947.6	2.0	1148.9	2.2	1552	3.5	41.8
GB1 377/24	1	413	0.3	1.1	3468.0	1.7901	0.0056	0.14071	0.00036	0.092	0.00013	0.9	848.7	2.0	1041.9	2.0	1473	2.7	45.2
GB1 379/13	8	71	0.3	3.5	1622	2.1274	0.0062	0.15645	0.00033	0.099	0.00016	0.8	937.0	1.9	1157.7	2.0	1598	3.0	44.4

Table 3. ID-TIMS U-Pb data

					Isotope ratios								Ages (Ma)						
No.	**Weight**	**U**	**Th/U**	**Pbc.**	**^{206}Pb/ ^{204}Pb**	**^{207}Pb/ ^{235}U**	**2 σ**	**^{206}Pb/ ^{238}U**	**2 σ**	**^{207}Pb/ ^{206}Pb**	**2 σ**	**Rho**	**^{206}Pb/ ^{238}U**	**2 σ**	**^{207}Pb/ ^{235}U**	**2 σ**	**^{207}Pb/ ^{206}Pb**	**2 σ**	**Disc. (%)**
	(ug)	(ppm)		(pg)															
CR-08-7.1	1	750.4	0.59	1.16	9971.1	3.187	0.017	0.24637	0.00125	0.0938	0.00008	0.99	1419.7	na	1453.9	na	1504.3	na	na
CR-08-7.2	26	170	0.55	2.59	26009.3	3.1265	0.0075	0.24289	0.00051	0.0934	0.00006	0.96	1401.7	na	1439.2	na	1495.1	na	na
CR-08-7.3	7	232.2	0.46	1.83	13048.7	2.9534	0.0068	0.23468	0.00047	0.0913	0.00007	0.95	1359.0	na	1395.7	na	1452.3	na	na
CR-08-7.4	3	317.5	0.46	2.91	4645.6	2.775	0.017	0.2255	0.00014	0.0893	0.00024	0.90	1310.8	na	1348.8	na	1409.7	na	na
CR-08-7.5	6	397.7	0.43	2.58	12578.7	2.6203	0.0060	0.21651	0.00043	0.0878	0.00006	0.95	1263.4	na	1306.3	na	1377.6	na	na
CR-08-7-2 390/15	1	63.1	0.48	1.28	763.4	3.1005	0.02590	0.24062	0.00121	0.0935	0.00057	0.3	1389.9	6.3	1432.8	6.4	1497.1	11.5	8.0
C-08-4 360/9	41	446.5	0.47	8.33	21827.9	1.5643	0.0037	0.15848	0.00033	0.0716	0.00005	0.96	948.3	1.8	956.2	1.5	974.2	1.3	2.9
C-08-4 360/10	13	391.9	0.60	1.48	35079.2	1.6144	0.0036	0.16290	0.00032	0.0719	0.00005	0.96	972.9	1.8	975.8	1.4	982.4	1.3	1.0
C-08-4 285/15	14	505.0	0.48	39.80	1661.3	1.4434	0.0043	0.14775	0.00033	0.0709	0.00012	0.83	888.3	1.8	906.3	1.8	950.4	3.5	7.0
C-08-4 285/54	4	695.2	0.86	6.63	4088.5	1.5239	0.0039	0.15485	0.00033	0.0714	0.00007	0.93	928.1	1.8	939.2	1.6	965.4	2.0	4.2
C-08-4 285/19	7	425.6	0.69	7.76	3633.3	1.4715	0.0038	0.15030	0.00032	0.0710	0.00007	0.92	920.7	1.8	918.0	1.6	954.9	2.1	5.9
C-08-4-3	1	236.5	0.52	1.4	1996.4	1.9960	0.0113	0.18380	0.00101	0.0788	0.00026	0.87	1087.7	5.5	1114.1	4.5	1166.1	6.4	7.3
C-06-3 172/5	13	135.6	0.56	2.49	9985.8	2.9252	0.0074	0.22520	0.00051	0.0942	0.00008	0.94	1309.3	2.7	1388.5	1.9	1512.3	1.6	14.8
C-06-3 172/6	22	113.2	0.53	2.60	14044.6	3.0515	0.0078	0.23378	0.00053	0.0947	0.00007	0.95	1354.3	2.8	1420.6	1.9	1521.5	1.5	12.2
C-06-3 172/4	23	81.5	0.64	2.24	12999.3	3.2615	0.0073	0.24810	0.00049	0.0953	0.00007	0.95	1428.6	2.5	1471.9	1.8	1534.9	1.3	7.7
C-06-3-1	5	88.0	0.40	2.68	1807.9	2.1885	0.0075	0.17432	0.00038	0.0911	0.00021	0.76	1035.9	2.1	1177.4	2.4	1447.8	4.3	30.8
C-06-3-3	1	237.7	0.41	1.39	2553.9	3.0987	0.0161	0.23633	0.00109	0.0951	0.00020	0.92	1367.6	5.7	1432.4	4.0	1529.9	3.9	11.8
743-03 69/13	271	178.8	0.82	17.70	8032.0	0.3365	0.0008	0.04674	0.00010	0.0522	0.00004	0.95	294.4	na	294.5	na	294.8	1.8	na
743-03 69/14	287	na	0.69	13.46	9294.0	na	na	na	na	0.0522	0.00006	na	na	na	na	na	292.2	2.5	0.9
743-03 77/11	171	203.2	0.70	5.08	20055.1	0.3370	0.0011	0.04676	0.00015	0.0523	0.00006	0.94	294.6	na	294.9	na	297.3	2.6	-0.7
743-03 77/2	212	238.7	0.84	16.70	8896.6	0.3363	0.0017	0.04676	0.00025	0.0522	0.00015	0.84	294.6	na	294.4	na	292.7	6.7	2.2
743-03 82/9	21	161.8	0.51	2.84	3499.9	0.3357	0.0030	0.04653	0.00041	0.0523	0.00018	0.92	293.2	na	293.9	na	299.7	8.1	0.1
743-03 82/10	214	448.4	1.26	17.35	16113.6	0.3342	0.0010	0.04646	0.00013	0.0522	0.00004	0.97	292.7	na	292.8	na	293.0	1.6	0.6

743-03 110/50	39	152.4	0.59	1.21	14368.7	0.3357	0.0008	0.04662	0.00010	0.0522	0.00005	0.91	293.8	0.6	293.9	0.6	295.4	2.2	1.3
743-03 110/49	188	157.7	0.76	2.48	34825.9	0.3348	0.0008	0.04647	0.00011	0.0523	0.00004	0.96	292.8	0.7	293.2	0.6	296.6	1.7	na
743-03-1 390/17	17	103.1	0.46	1.75	2924.6	0.3328	0.0012	0.04637	0.00010	0.0521	0.00014	0.68	292.2	0.6	291.7	0.9	287.8	6.2	-1.6
743-03-2 390/18	1	1993.4	1.04	2.66	2218.0	0.3372	0.0030	0.04691	0.00038	0.0521	0.00016	0.94	295.5	2.3	295.0	2.2	291.1	6.9	-1.5
743-03-4 390/20	1	467.4	0.71	0.83	2090.3	0.4200	0.0029	0.05849	0.00030	0.0521	0.00021	0.81	366.4	1.9	356.1	2.1	289.2	9.2	-27.5
743-03-5 390/21	1	595.6	0.60	0.83	2085.7	0.3296	0.0017	0.04590	0.00012	0.0521	0.00021	0.65	289.3	0.8	289.2	1.3	288.5	9.2	-0.3
S2/ZIR1	31	164.0	0.28	40.90	1843.2	2.9120	0.0679	0.23458	0.00601	0.0900	0.00102	0.90	1358.4	na	1385.0	na	1426.3	na	na
S2/ZIR5	4	164.0	0.28	6.33	1505.5	2.8193	0.0193	0.22928	0.00139	0.0892	0.00021	0.94	1330.7	na	1360.7	na	1408.1	na	na
S2-2	2	112.0	0.34	1.25	2742.6	3.1411	0.0146	0.24282	0.00086	0.0938	0.00025	0.82	1401.4	4.5	1442.8	3.6	1504.5	5.0	7.6
S2-3	1	468.5	0.39	1.03	6686.2	2.8820	0.0089	0.23428	0.00063	0.0892	0.00010	0.93	1356.9	3.3	1377.2	2.3	1408.8	2.2	4.1
STANG4-2	1	616.7	0.21	1.80	4499.6	2.4126	0.0129	0.20909	0.00104	0.0837	0.00012	0.96	1224.0	5.6	1246.4	3.8	1285.3	2.8	5.2
STANG4-3	1	277.0	0.43	1.93	2345.9	3.3784	0.0155	0.25892	0.00103	0.0946	0.00019	0.90	1484.3	5.3	1499.4	3.6	1520.8	3.7	2.7
STANG4-4	1	221.3	0.53	1.28	2848.1	3.4293	0.0123	0.26149	0.00075	0.0951	0.00017	0.86	1497.5	3.8	1511.1	2.8	1530.3	3.4	2.4
BR.-1	1	477.2	0.38	1.3	4507.1	2.0620	0.0071	0.19126	0.00053	0.0782	0.00013	0.88	1128.2	2.9	1136.3	2.4	1151.8	3.3	2.2
BR.-2	2	156.9	0.24	63.8	71.9	1.8618	0.0790	0.17286	0.00140	0.0781	0.00326	0.19	1027.8	7.7	1067.6	27.6	1149.8	80.6	11.5
BR.-3	4	189.1	0.34	19.0	491.6	2.0421	0.0116	0.18958	0.00050	0.0781	0.00037	0.55	1119.1	2.7	1129.7	3.9	1150.0	9.4	2.9
BR.-4	79	118.6	0.37	7.4	15789.9	2.1689	0.0081	0.19844	0.00055	0.0793	0.00015	0.88	na	na	na	na	1178.9	3.7	1.1
BR.-5	79	118.7	0.38	6.5	17985.3	2.1740	0.0048	0.19868	0.00042	0.0794	0.00006	0.94	na	na	na	na	1181.2	1.5	1.2
BR.-6	76	105.3	0.40	10.6	9355.5	2.1348	0.0045	0.19686	0.00037	0.0787	0.00005	0.96	na	na	na	na	1163.4	1.2	0.5
BR.-7	128	132.8	0.42	7.2	29192.3	2.1217	0.0051	0.19638	0.00044	0.0784	0.00005	0.97	na	na	na	na	1156.0	1.2	0.0
BR.-8	128	132.7	0.42	6.3	32951.2	2.1222	0.0046	0.19644	0.00040	0.0784	0.00005	0.95	na	na	na	na	1155.9	1.3	0.0
BR.-9	97	125.5	0.42	24.9	6043.7	2.1263	0.0061	0.19693	0.00053	0.0783	0.00005	0.97	na	na	na	na	1154.7	1.3	-0.4
BR.-10	3	72.4	0.40	0.7	3593.6	2.1112	0.0102	0.19578	0.00083	0.0782	0.00016	0.91	na	na	na	na	1152.3	4.0	0.0
BR.-11	9	96.8	0.42	2.2	4739.8	2.0872	0.0086	0.19376	0.00069	0.0781	0.00014	0.91	na	na	na	na	1150.1	3.4	0.8
BR.-12	1	175.0	0.35	0.6	3298.6	2.0675	0.0124	0.19258	0.00100	0.0779	0.00019	0.91	na	na	na	na	1143.4	4.9	0.8
BR.-13	3	48.7	0.38	1.5	1184.1	2.0683	0.0152	0.19149	0.00101	0.0783	0.00035	0.80	na	na	na	na	1155.4	8.8	2.4

FCT-2	1	1082.3	0.53	0.98	324.9	0.0288	0.0008	0.00444	0.00006	0.0470	0.00117	0.53	28.6	0.4	28.8	0.8	50.3	58.8	43.4

Table 4. U-He and U-Pb data

Sample	He, cc	U,ng	Th,ng	Th/U	Age (Ma)	Error (Ma)	Ft	Corrected Age (Ma)	$^{206}Pb/^{238}U$ (Ma)	$^{207}Pb/^{235}U$ (Ma)	$^{207}Pb/^{206}Pb$ (Ma)
Ne-syenite - Larvik											
743-3-1	1.27E-07	1.741	0.80163	0.460442	517.88	249.7	0.87	597.77	292.2	291.7	287.8
743-3-2	1.19E-07	1.979	2.064313	1.043109	385.96	1.93	0.77	499.86	295.5	295.0	291.1
743-3-4	1.70E-08	0.464	0.332108	0.71575	252.23	37.19	0.77	326.66	366.4	356.1	289.2
743-3-5	3.45E-08	0.591	0.357419	0.60477	406.31	5.69	0.77	526.22	289.3	289.2	288.5
Augengneiss - Gjærsøen											
S2-3	1.26E-08	0.465	0.180682	0.388563	200.67	44.53	0.67	301.02	1356.9	1377.2	1408.8
Orthogneiss - Nevlunghavn											
C-06-3-1	1.22E-08	0.437	0.177851	0.406982	205.35	3.61	0.72	284.45	1035.9	1177.4	1447.8
C-06-3-3	8.36E-09	0.236	0.097742	0.414159	259.61	1.45	0.65	398.43	1367.6	1432.4	1529.9
Granodioritic gneiss - Stangnes											
STANG4-3	1.80E-08	0.275	0.11897	0.432617	468.15	2.42	0.69	680.79	1484.3	1499.4	1520.8
STANG4-4	2.52E-08	0.22	0.11767	0.534865	781.29	264.62	0.66	1189.27	1497.5	1511.1	1530.3
Granite - Finse											
C-08-4-3	9.86E-09	0.235	0.123331	0.524814	299.25	242.38	0.63	476.39	1087.7	1114.1	1166.1
Augengneiss - Kvitenut											
CR-08-7-2	3.17E-09	0.063	0.030183	0.479098	360.7	2.89	0.54	672.31	1389.9	1432.8	1495.1
Porphyry - Brunkeberg											
BR.-1	2.03E-08	0.474	0.179846	0.379423	314.78	1.62	0.62	504.73	1128.2	1136.3	1151.8
BR.-2	9.56E-09	0.312	0	0	246.36	1.35	0.59	414.47	1027.8	1067.6	1149.8
Fish Canyon Tuff											
FCT 2	1.03E-09	1.075	0.80163	0.745702	6.98	10.93	0.76	9.15	28.6	28.8	50.3
Örœfajökull											
SAL 679 377/13	na	na	na	na	1132	113.2	na	na	690.8	832.7	1233.1
SAL 679 377/15	na	na	na	na	9.4	4.7	na	na	37.0	38.8	na
HVRT1 377/16	na	na	na	na	1.4	0.7	na	na	0.19	0.2	na
HVRT1 377/17	na	na	na	na	916	274.8	na	na	789.5	856.2	1032.9
SB1 377/19	na	na	na	na	1.7	0.34	na	na	0.0	-0.2	na

SB1 377/20	na	na	na	na	18.2	18.2	na	na	0.2	-2.8	na
SB1 377/21	na	na	na	na	3.3	3.3	na	na	0	0.1	na
GB1 377/22	na	na	na	na	99	49.5	na	na	-0.8	-20.9	na
GB1 377/23	na	na	na	na	1250	125.0	na	na	947.6	1148.9	1551.7
GB1 377/24	na	na	na	na	1070	107.0	na	na	848.7	1041.9	1473.0

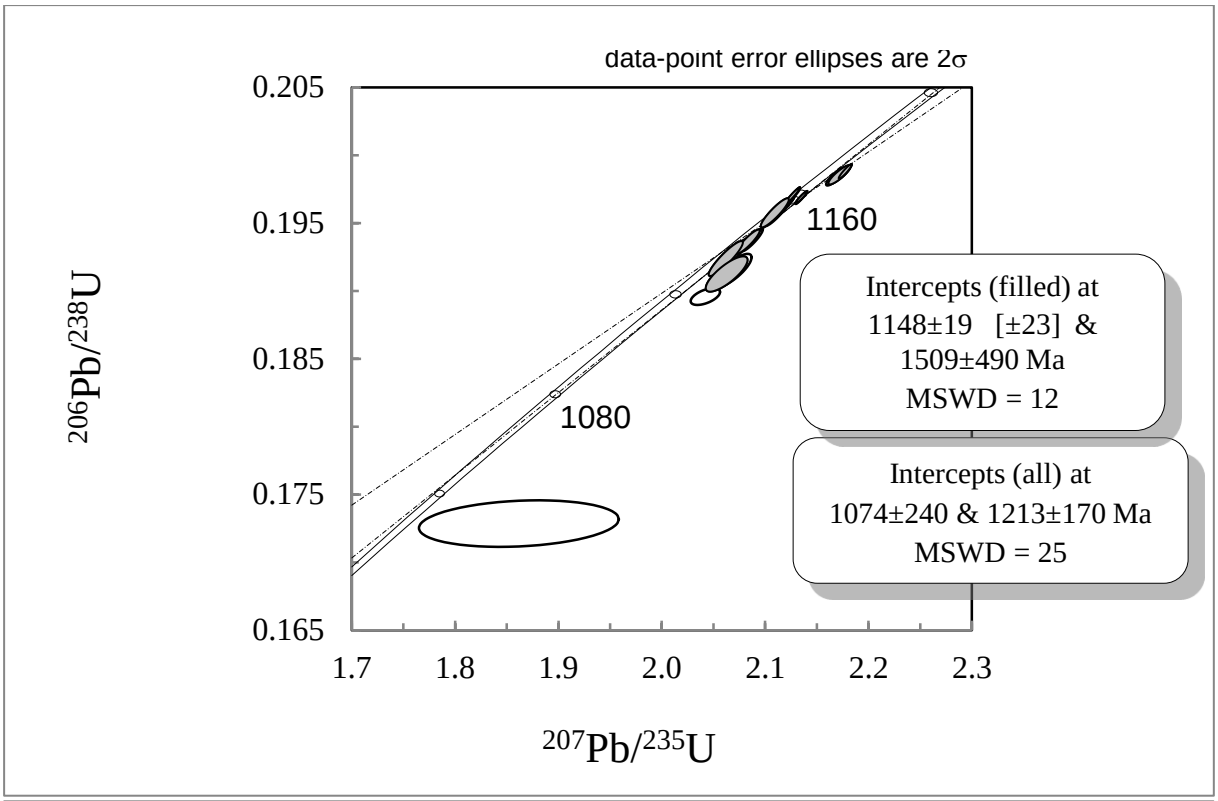

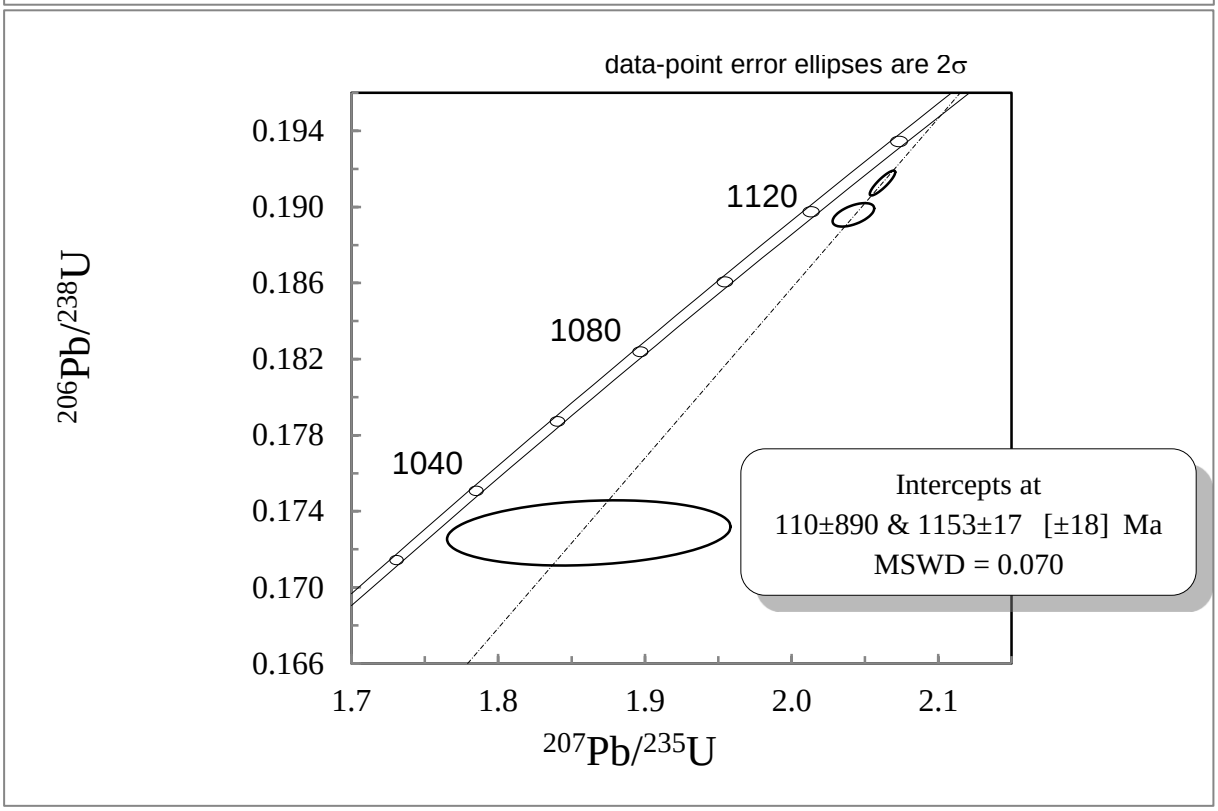

Figure 17a-b. Concordia diagram for BR, Brunkeberg. Fig. 17a show the old data plotted as filled ellipses, whereas the open ellipses are new data points. In fig. 17b only the new data points are plotted.

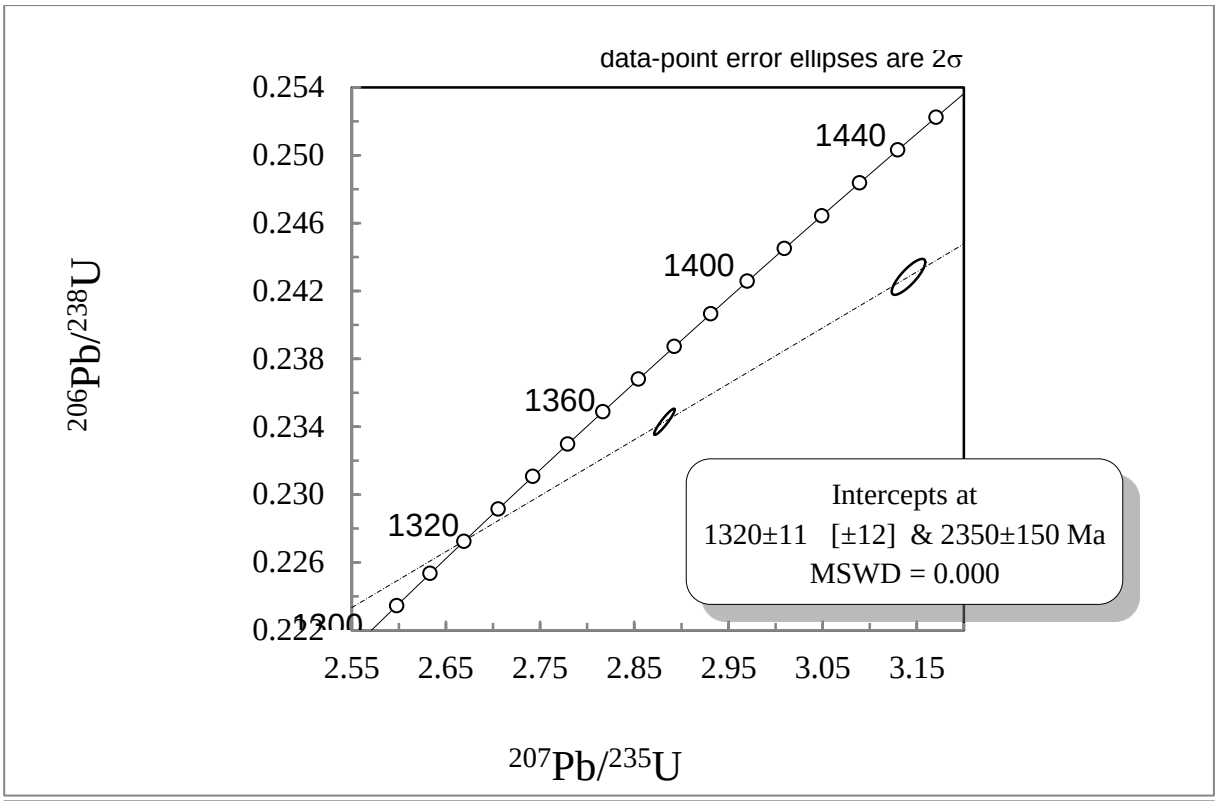

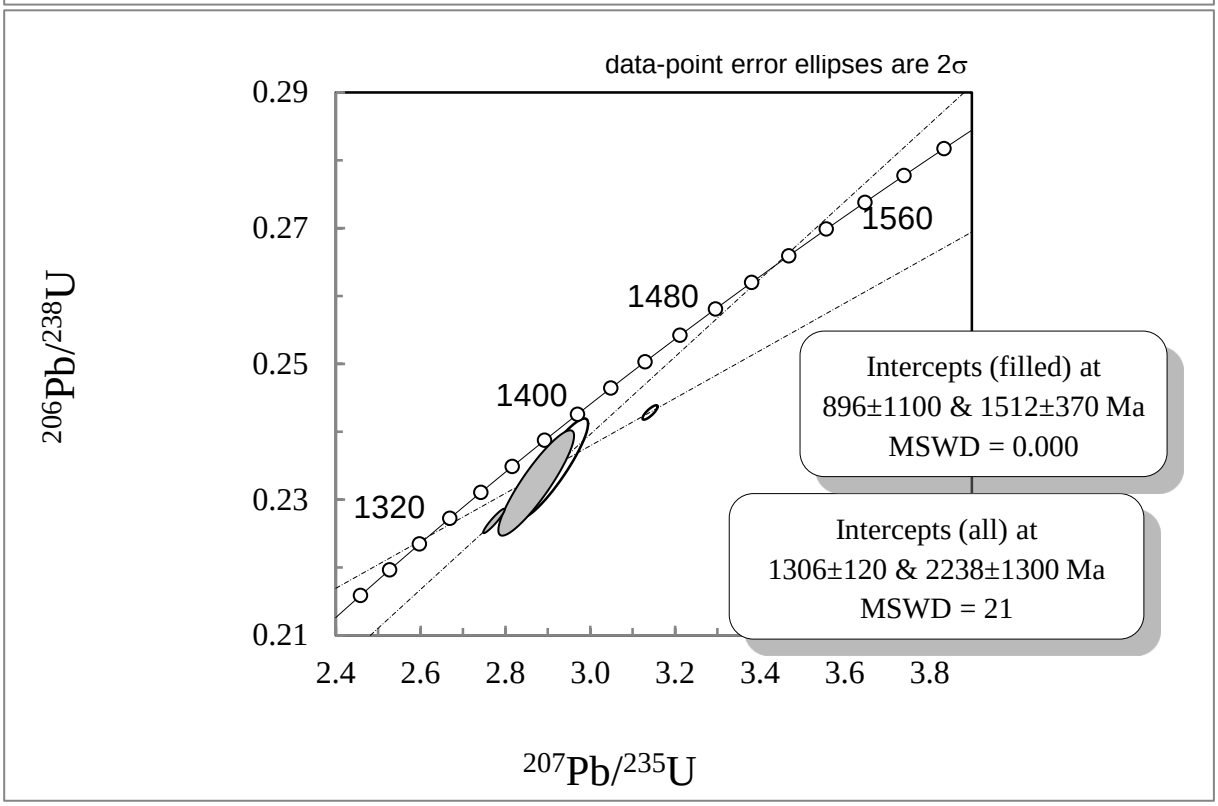

Figure 18a-b. Concordia diagram for sample S2, Gjersjøen. Error ellipses are 2σ. In fig. 18a, regression lines for the old data points and all of the data points together are shown. In fig. 18b, points and regression line for the new data is shown.

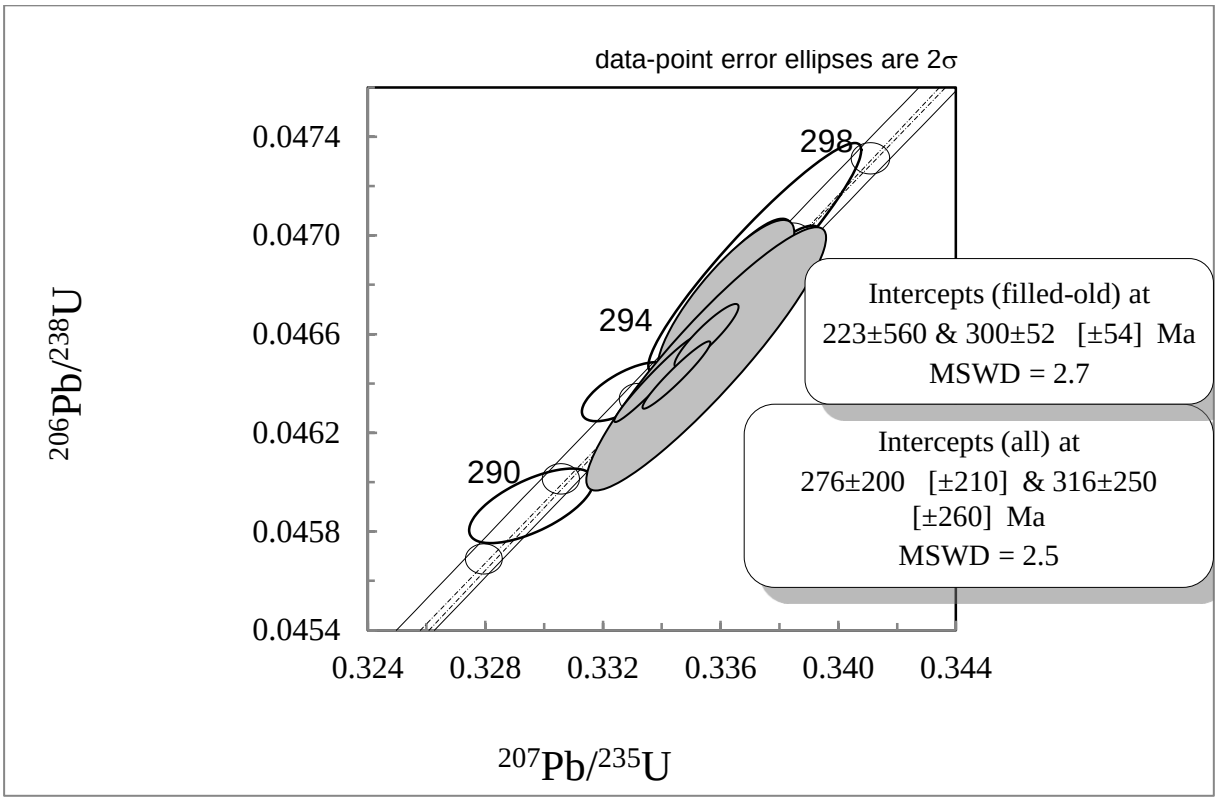
data-point error ellipses are 2σ
0.0474
0.0470
0.0466
0.0462
0.0458
0.0454
298
294
290
Intercepts (filled-old) at
223±560 & 300±52 [±54] Ma
MSWD = 2.7
Intercepts (all) at
276±200 [±210] & 316±250
[±260] Ma
MSWD = 2.5
0.324
0.328
0.332
0.336
0.340
0.344
206Pb/238U
207Pb/235U

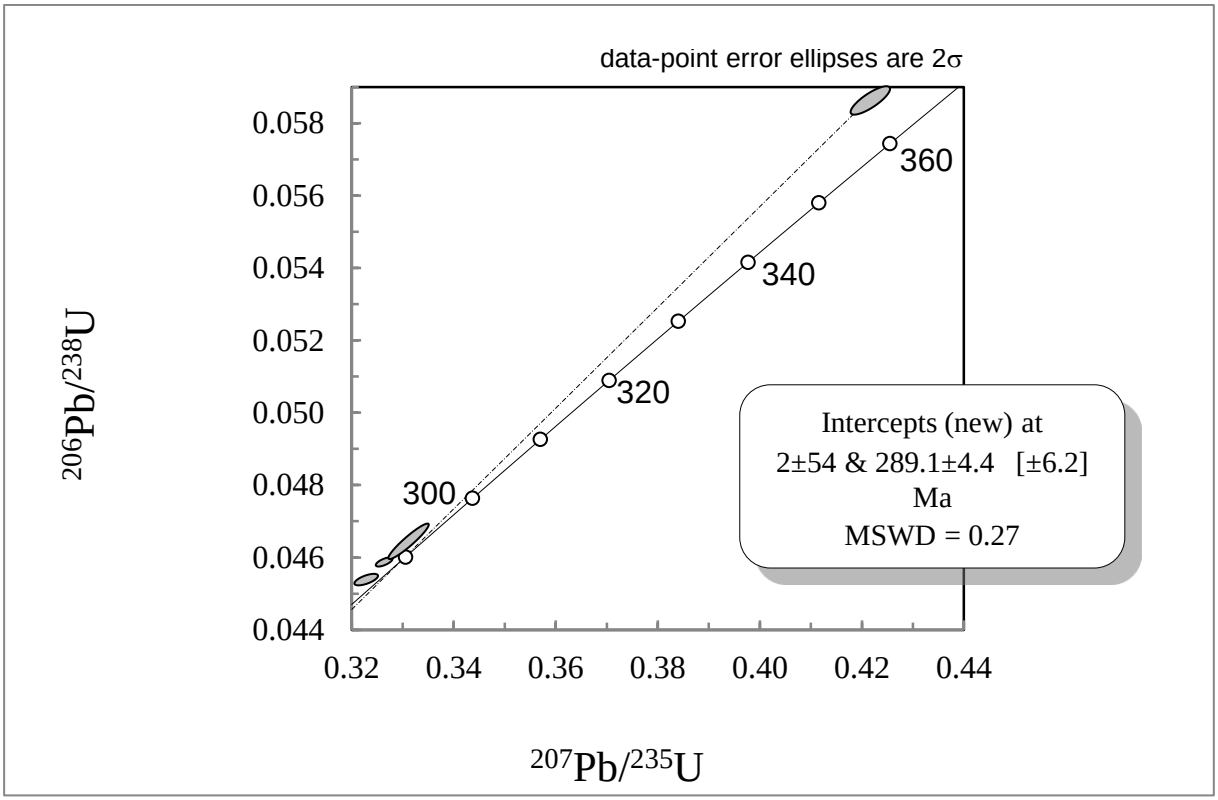
data-point error ellipses are 2σ
0.058
0.056
0.054
0.052
0.050
0.048
0.046
0.044
360
340
320
300
Intercepts (new) at
2±54 & 289.1±4.4 [±6.2]
Ma
MSWD = 0.27
0.32
0.34
0.36
0.38
0.40
0.42
0.44
206Pb/238U
207Pb/235U

Figure 19a-b. Concordia diagram for sample 743-03 from Larvik. Error ellipses are 2 σ. In fig. 19a filled ellipses are old data points, whereas the open ellipses are new data points. Fig. 19b shows only new data points.

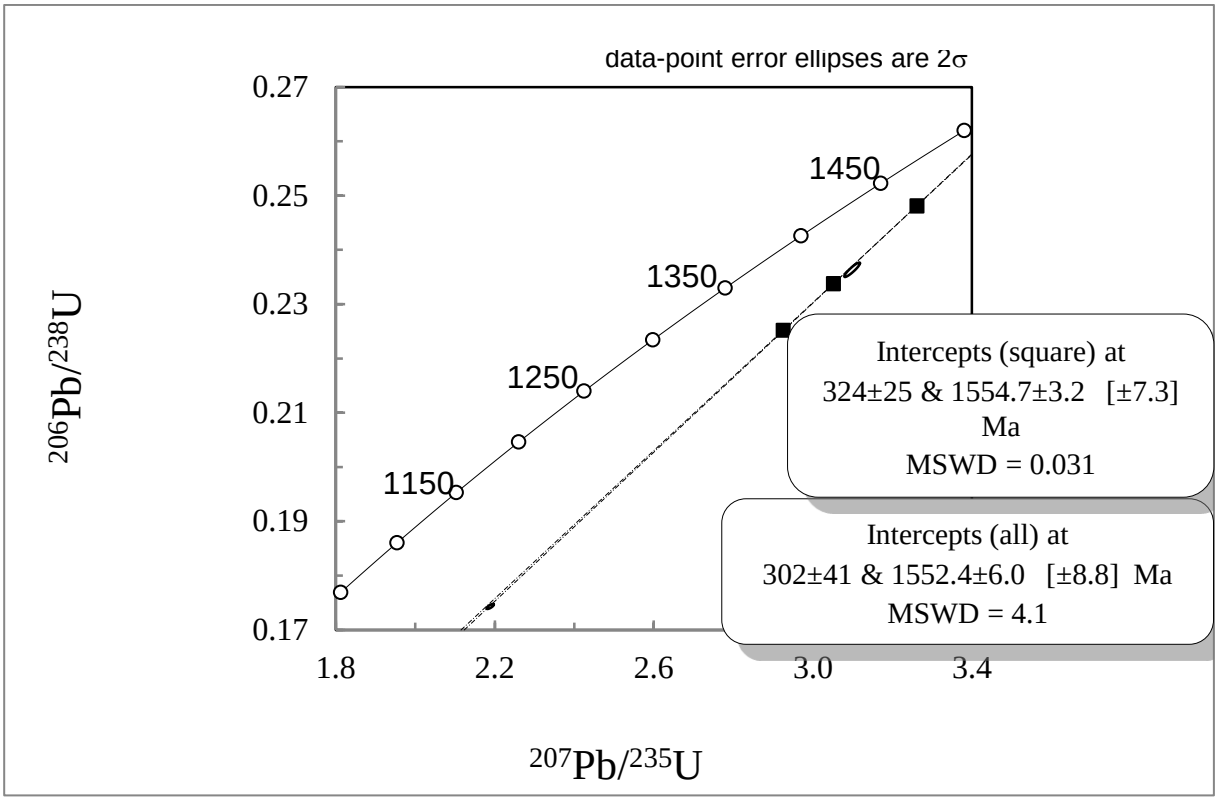

Fig. 20. Concordia diagram for sample C-06-3. The three black squares represent the old point, while the two open ellipses represent the new points.

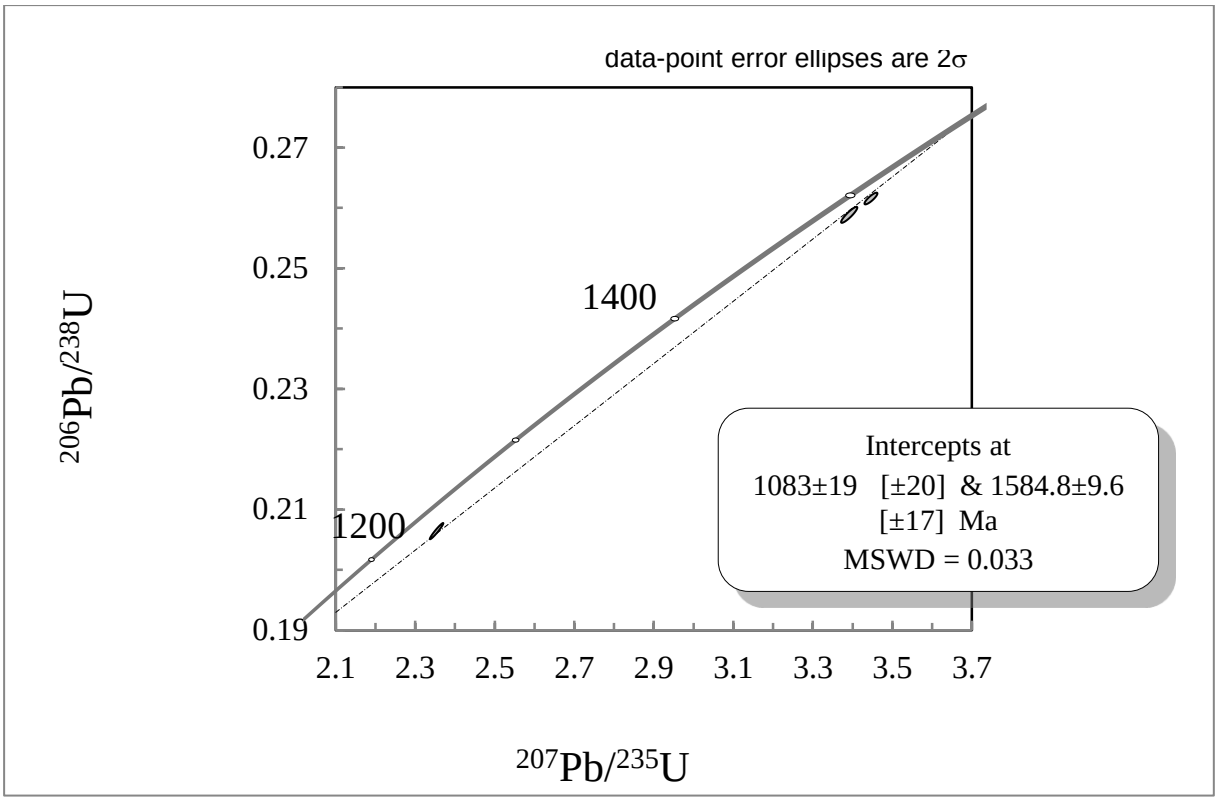

Fig.21. Concordia diagram for sample STANG4, Stangnes. For detailed description, see text.

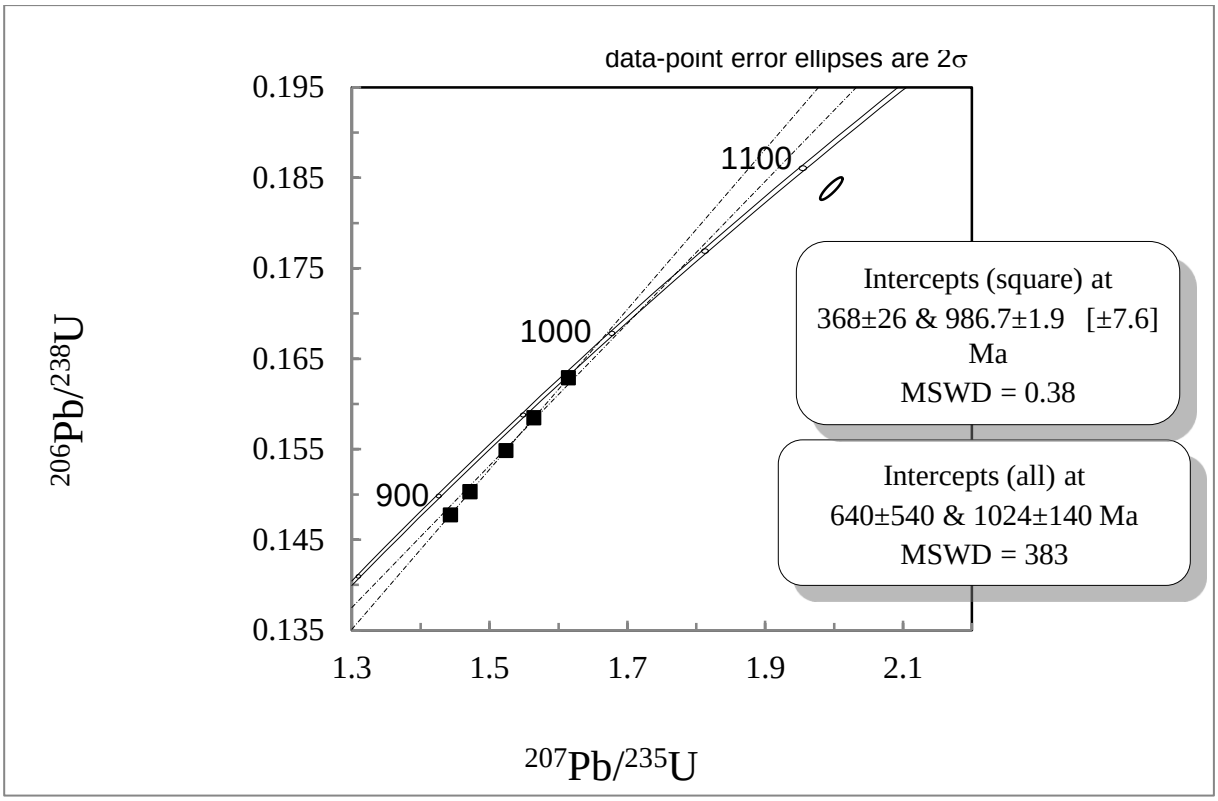

Figure 22. Concordia diagram for sample C-08-4, Finse. The black squares old data points, whereas the open ellipse is a new point. For detailed description, see text.

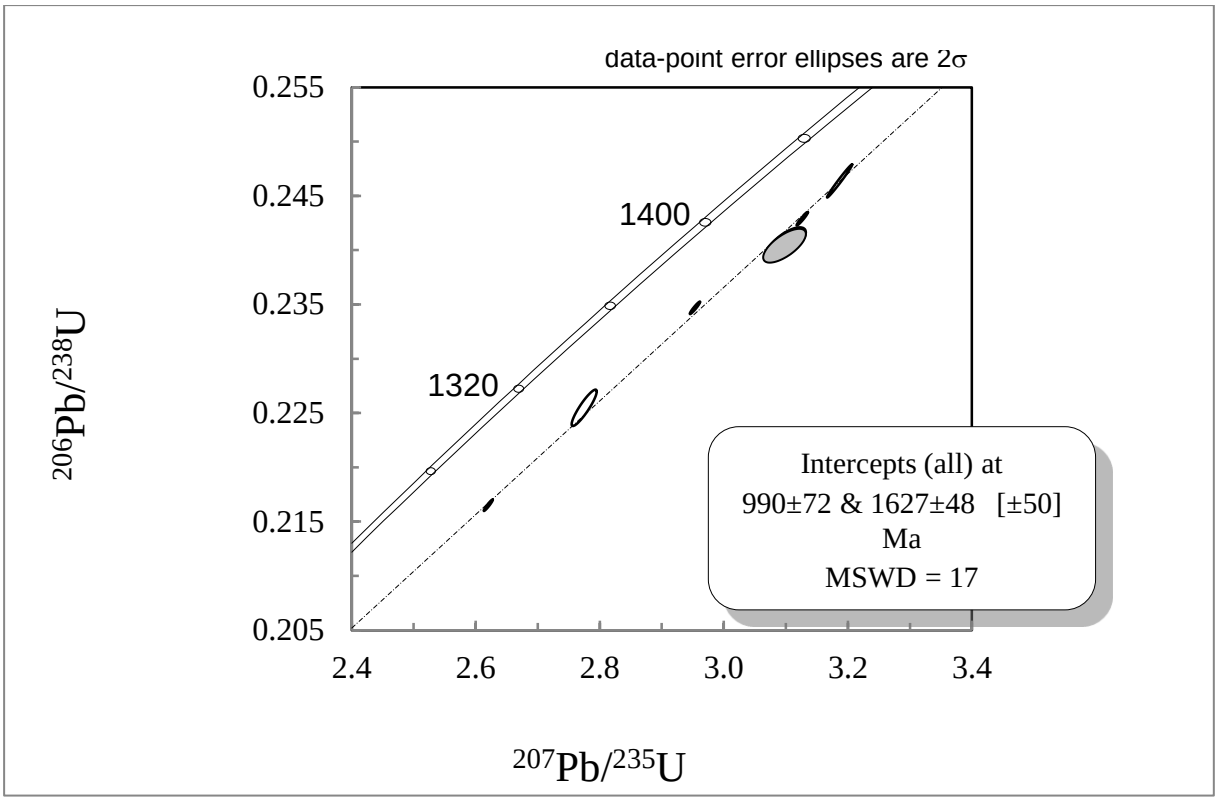

Figure 23. Concordia diagram for CR-08-7, Kvitenut. The filled error ellipse represents the newly added datapoint.

5. Discussion

5.1 U-Th-He ages: technical aspects

He extraction

A wide range of He re-extraction abundances were achieved within and between the measured samples. The larvikite sample, 743-3, varied from 0.1 – 9.9 %, whereas C-08-4-3 from Nevlunghavn yielded a reheating abundance of 17.8 %. The rest of the samples varied from 0.1 – 5.9 %. These wide ranges of reheating abundances reflect the time spend heating, the temperature of the heated Pt-capsules and the retentivity of He in the zircon grains. The power was increased during heating until the colour on the monitor showed that the sample had reached the wanted temperature of 1100 - 1300°C. The power needed to heat up the capsules, ranged from 40 – 57 % of maximum power. A slightly different geometry for each capsule (i.e. the way the capsule was enclosed), giving different areas radiated by the laser, might have contributed to these differences, although it is most likely that differences in temperature for the heated capsules would affect the efficiency of the He extraction.

C-06-3 - Nevlunghavn

During heating of the sample C-06-3-3, the Pt-capsule melted partly. The melting point of Pt is about 1770°C, whereas zircon decomposes to ZrO_2 and SiO_2 at 1673°C before eutectic melting of the ZrO_2-SiO_2-assemblage at 1687°C (Kaiser et al., 2008). The partial melting could possibly have resulted from a short laser power surge or from micro scale impurities in the Pt-capsule. In this case the zircon suffered no visible damage. Crystal grains not enclosed in Pt tubes during heating with the laser, however, may loose U and Th, presumably by volatilization (Reiners and Farley, 1999), and might cause He ages to be erroneously high. A partial loss of U might explain the discrepancy in He ages between C-06-3-1 and C-06-3-3, giving ages of 284.45 ±3.61 Ma and 398.43 ±1.45 Ma, respectively. The age achieved for C-06-3-1 is, therefore, more reliable.

Fish Canyon Tuff

The inconsistent FCT zircon grain giving a U-He age of 9.15 Ma (instead of ca 28 Ma, e.g. Foeken et al., 2006) had a reheating abundance of 58% compared to the first heating step, several times higher than the 1 – 10% for all other measured zircons. The amount of He reported by Foeken et al. (2006) for FCT, ranges from 4.31E-09 to 1.17E-08 cc. The amount measured for FCT2 is 1.03E-09 cc, about ¼ of the lowest abundance reported Foeken et al. (2006). A loss of He during the first step of measurement, would give rise to an artificial high reheating abundance, and could potentially explain the low amount of He and low (U-Th)/He age.

Tagami et al. (2003) reports anomalously low He ages for a FCT zircon grain of 16.6 and 14.1 Ma after alpha ejection correction, even though several heating steps were performed for the latter zircon. As seen in figure 1, the abundance of He released in each step for the zircon FCTZr-S1 is relatively low, and up to seven steps of heating were needed to get the amount of He extracted in the final heating step to below 1 % of the accumulated amount. The U-He age of 9.15 Ma from FCT2 (table x) is c. 2/3 of the anomalously low Fish Canyon Tuff reported by Tagami et al. (2003). The authors give no explanation for the high retentivity for FCTZr-S1; however, it is unlikely that the same effect(s) could explain the even lower He age of FCT 2, given the high amount of reheating at 36.8 % of the accumulated helium. The third step of heating gave a reheating of 0.7 % of the total accumulated.

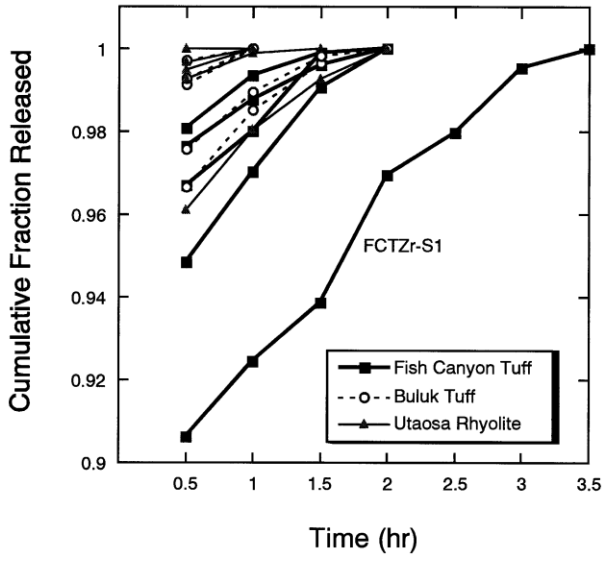

Figure 24. Cumulative fraction released normalized to total ^{4}He. Each step was heated at 1300°C for 30 min each. See text for detailed description. Adopted from Tagami et al. 2003.

STANG4-4

The samples STANG4-3 and STANG4-4 yielded ages of 680.79 ±2.42 Ma and 1189.27 ±264.62 Ma, respectively. The high uncertainty of STANG4-4, the quite high age difference between STANG4-3 and STANG4-4 (c. 509 Ma) and the uncertainty of calculating the correction for alpha ejection makes this age fairly unreliable. A slow cooling history could account for some of the discrepancy between the U-He ages, although the peak amphibolite facies represented by the lowermost interception on the Concordia curve at 1083.19 ±19 Ma, indicates that the temperature reached at least 500°C. It is unrealistic that the He would be retained at this temperature, especially if the cooling was slow. STANG4-3 with an age of 680.79 ±2.42 Ma is therefore more reliable.

5.2 Comparison of U-Pb and U-Th-He ages

The Precambrian zircon grains measured for He by F.Stuart at SUERC and U-Th-Pb by F.Corfu yielded similar Precambrian ages (see table 4).
By comparing the xenocrystic zircons U-Pb and U-He ages with zircons from The Oslo Region and other areas that might be a source of contamination, it is possible to reduce the number of sources as potential suspects. None of the samples from southern Norway dated for this thesis (see table x) yielded positively overlapping U-He and U-Pb ages.

The locations for the newly gathered data for this thesis, together with a compilation of apatite, zircon and titanite fission track data for Fennoscandia from Hendriks et al. (2007), is given in figure Q. In Finland, the oldest AFT ages range from 543 to 900 Ma in Rumouvaara, whereas in Mid-Sweden ZFT ages as high as 853 – 929 Ma are recorded (Hendriks et al., 2007, and reference therein).

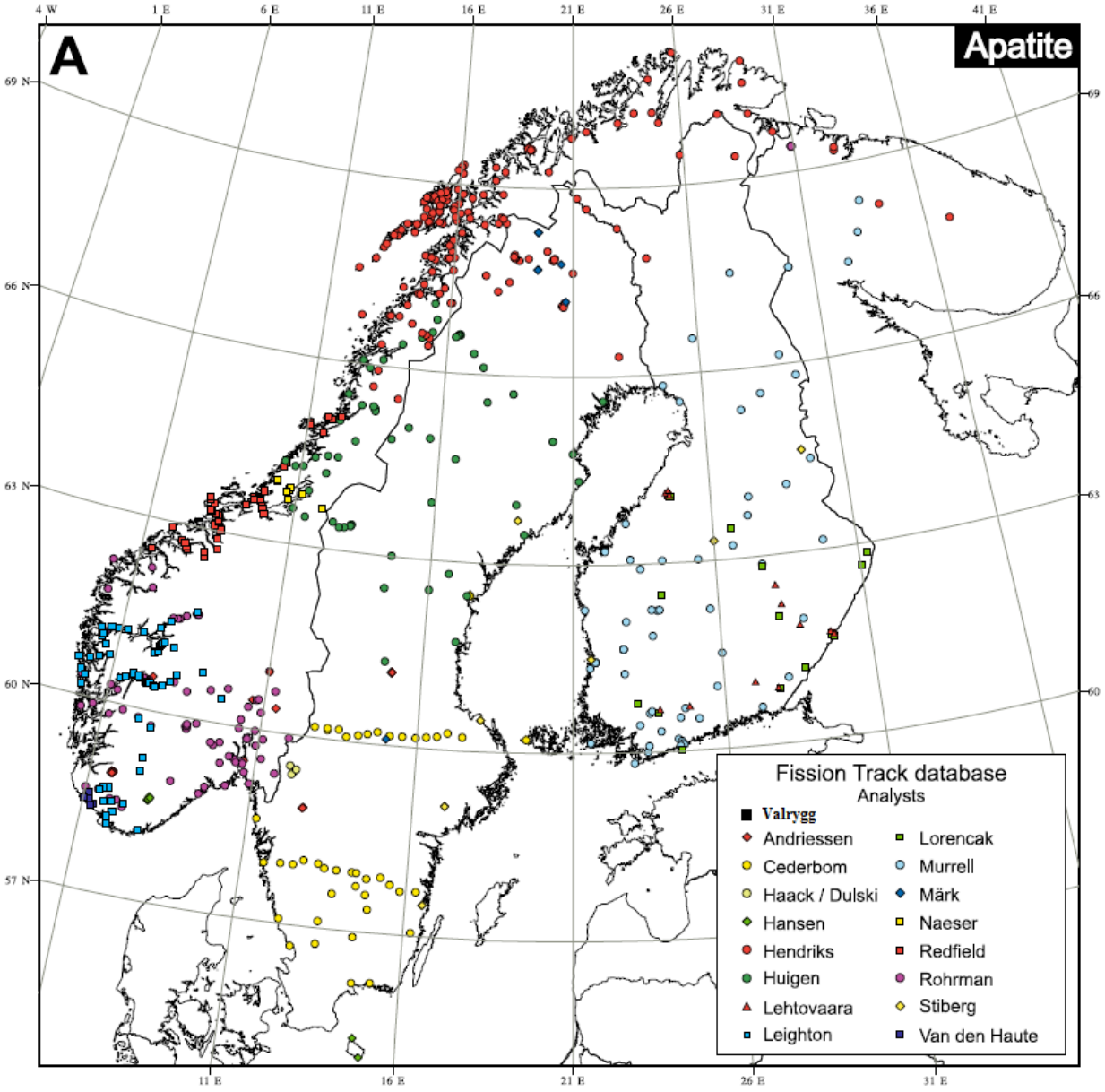
A
Apatite
4 W
1 E
6 E
11 E
16 E
21 E
26 E
31 E
36 E
41 E
69 N
66 N
63 N
60 N
57 N
Fission Track database
Analysts
Valrygg
Andriessen
Cederbom
Haack / Dulski
Hansen
Hendriks
Huigen
Lehtovaara
Leighton
Lorencak
Murrell
Märk
Naeser
Redfield
Rohrman
Stiberg
Van den Haute

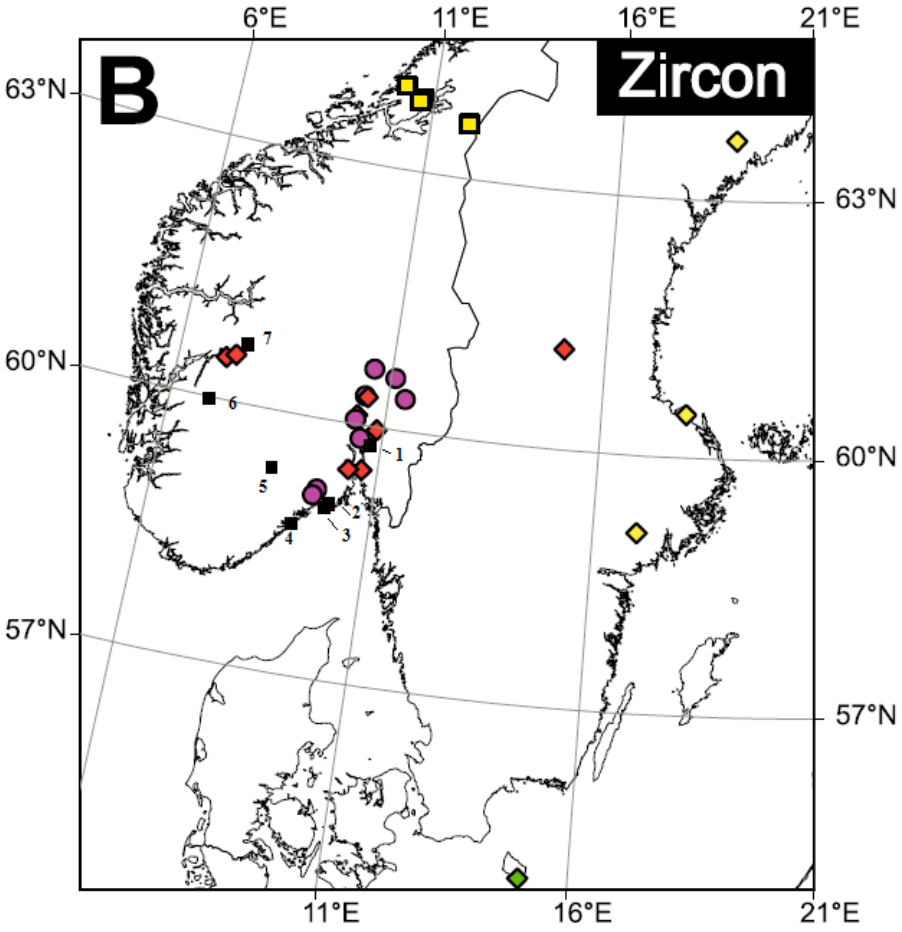
B
Zircon
6°E
11°E
16°E
21°E
63°N
60°N
57°N
1
2
3
4
5
6
7

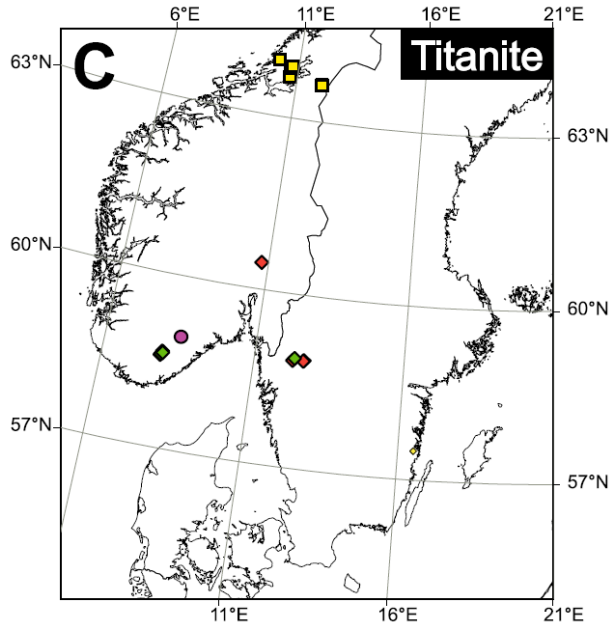
C
Titanite
6°E
11°E
16°E
21°E
63°N
60°N
57°N

Figure 25A-C. Simplified map showing fission track data for apatite (A), zircon (B) and titanite (C). The black squares in figure B. are zircon (U-Th)/He data gathered by Valrygg, showing: 1) S2 from Gjersjøen, 2) 743-3 from Larvik, 3) C-06-3 from Nevlunghavn, 4) STANG4 from Stangnes, 5) Br from Brunkeberg, 6) C-08-4 from Finse, and 7) CR-08-7 from Hardangervidda. Modified after Hendriks et al. 2007.

The Precambrian xenocrysts from Iceland match typical ages in the Proterozoic crust in East Greenland. Most of the rocks from East Greenland show AFT resetting after the Caledonian orogeny (e.g. Hansen and Brooks, 2002). However, AFT ages of 836 ±57 Ma, have been reported from the Kangertittivatsiaq area (Hansen and Brooks, 2002) and c.850 Ma, in the crystalline basement south of the Kangerlussuaq area (Hansen, 2000). The authors give no explanation for the abnormally high AFT ages. Titanite Fission track ages of 435 ±14 Ma and 413 ±10 Ma have been reported by Gleadow and Brooks (1979), representing the Caledonian orogeny. It is unknown if any of the fission track data from Greenland, Sweden or Finland correlates positively with their corresponding U-Pb ages. Although the FT ages in theory would be older than the corresponding U-He ages, the relatively old FT ages indicate that high U-He ages from zircon is to be expected, both in Greenland and Scandinavia. Based on the AFT data from Greenland, it is not possible to disregard that the xenocrystic zircons have their origins from the JMR.

5.3 U-Th-He ages – Norway

C-06-3 – Nevlunghavn and 743-3- Larvikite

The third stage of the formation of the Oslo Rift, associated with plateau lava and rifting, saw the intrusion of Larvikite between 292.1 Ma to 298.6 Ma (and later the Siljan-Skrim plutonic complex to the NNW of Larvik, dated at 281.2 Ma in the north of the complex and 277.3 Ma in the south (Pedersen et al., 1995). Given the uncertainty of alpha ejection correction (uncorrected age at 205.35 Ma), the unknown grade of zonation and an error of 3.61 Ma for the zircon C-06-3-1, the U-He age (284.45 Ma) seems to be in close correspondence to the intrusion of the Larvikite or Skrim plutonic complex. With a retention temperature of 240°C (Zaun and Wagner, 1985), zircon fission track ages are older than their respective U-He ages.

Rohrman et al. (1994) dated zircons from pre-rift sediments in Porsgrunn using fission tracks, getting a post-rift Triassic age of 228 ±22 Ma, suggesting complete annealing and

temperatures in excess of 240°C at that time. Within the larvikite pluton, apatite FT gives ages of 194 Ma. An underestimation of apatite FT ages in Fennoscandia as a result of annealing have been argued by Hendriks and Redfield (2005), although Green et al. (2006) argues for a change in the He retention properties of apatite to explain the underestimation. The partial annealing zone for apatite is c. 100°C (Naeser and Faul. 1969). An age difference of 90 Ma between zircon U-He age from Nevlunghavn and apatite FT age from the larvikite might be explained by "too low" AFT ages, an underestimation of the closure temperature for He diffusion or due to uncertainties from calculating the alpha ejection correction.
An age difference of 56 Ma between the zircon U-He age in Nevlunghavn (284.45 Ma) and zircon FT age in Porsgrunn (228 Ma) would suggest large thermal differences within a distance of c. 25 km.

S2 – Gjersjøen

The uncorrected U-He age for the sample S2 from Gjersjøen in Kolbotn is 200.67 Ma, whereas the corrected is 301.02 Ma ±44.53. Rohrman et al. (1994) dated an apatite by fission tracks in Ski, c. 8 km south of Gjersjøen, getting an age of 176 ±21 Ma. Although there is a high uncertainty in the sample from Gjersjøen and a lack of correction for zonation, the age seem to be too high. The argumentation follows the same as for C-06-3 with possible low APF ages, overestimation by alpha ejection or an underestimation for the closure temperature for helium diffusion in zircon.

Brunkeberg – Telemark

The U-He ages for BR.-1 and BR.-2 are 504.73 ±1.6 and 414.47 ±1.4 Ma, respectively, and probably reflects the Caledonian Orogeny. However, Oscillary zoning and longitudinal zonation have been reported (Lajooki et al. 2002), and might have affected the alpha ejection correction. Rohrman et al. (1994), however, reports of AFT ages from 128 ±16 Ma to 239 ±22 Ma. This high discrepancy between U-He and AFT ages could reflect a slow cooling rate and/or thermal differences within the region.

STANG4 – Stangnes

The U-He age of the zircon STANG4-3 is 680.79 ±2.42 Ma, and is the highest U-He age measured in this study. Titanite fission track ages reported by Rohrman et al. (1994), range from 468 ±30 Ma in a Precambrian amphibolite to 665 ±45 Ma in a Precambrian Skarn. Titanite has a closure temperature of c. 300°C (Naeser and Faul. 1969), and should therefore be older than the U-He ages for zircons. A slow cooling rate might explain this age discrepancy. The high U-He and titanite FT ages, indicate that the flank of the Oslo Rift have not experienced thermal resetting in Carboniferous or Permian (Rohrman et al., 1994).

C-08-4 – Finse

The U-He-age for C-08-4 of 476.39 ±242.38 Ma is in close correspondence with the Caledonian orogeny, however, with a high uncertainty. Figure 26 shows a trend with ages get younger towards the inland. See figure 25, point 6 for comparison. Although the age of C-08-4 matches the Caledonian Orogeny, it is not clear why there is such a large discrepancy between the U-He age from this zircon and AFT reported in Hendriks et al. 2007. There is also a large age difference from within Hardangervidda, when comparing U-He ages with the sample from Kvitenut.

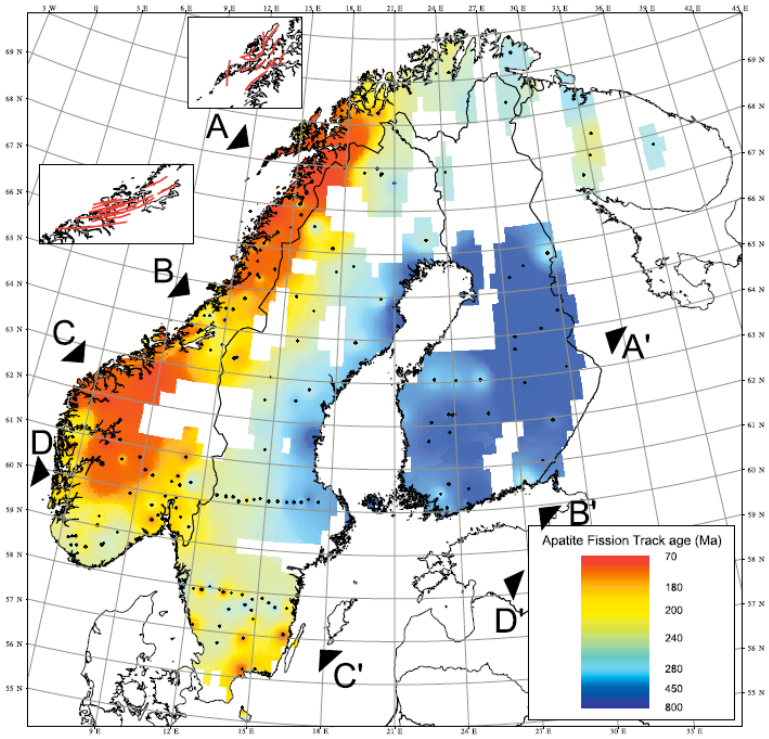

Figure 26. Map showing apatite fission track ages in Fennoscandia. Figure from Hendriks et al. 2007.

CR-08-7 – Kvitenut

The U-He age for CR-08-7-2 without alpha ejection correction is 360.7 ±2.89 Ma and 672.31 Ma after the correction. This zircon is the smallest measured with a length of about 100 µm and a half-width of about 25 µm, giving a Ft (for alpha correction) of 0.54. Roffeis et al. (2013) argue that the zircons from the Kvitenut Nappe have not been strongly affected by the Caledonian Orogeny, in agreement with the U-He age achieved by this study.

5.4 Abnormally high He ages

Tagami et al. (2003) reports He ages as much as 35 % higher than the U-Pb age for a Tardree Rhyolite zircon when corrected for alpha ejection. The raw age before the correction is in closer agreement, being about 4 % lower than the known age. They attribute this anomalously old age to a strong zonation, with a high U content in the core and low content at the rim.

Reiners et al. (2002) achieved consistent He ages for the quickly cooled Fish Canyon Tuff zircon, whereas more slowly cooled samples such as Gold Butte shows that other factors than temperature might influence He retentivity, suggesting the existence of a range of diffusion domains or ongoing annealing of radiation damage. Reiners et al. (2004), however, compares zircon He ages with K-feldspar $^{40}Ar/^{39}Ar$ models, which tend to agree quite well, and concludes that the departures from linearity in early stages of Arrhenius arrays are insignificant for bulk closure temperature.

The alternative is that He is retained at higher temperatures than previously achieved during step heating experiments (e.g. Reiners et al., 2002). Reich et al. (2007) shows through empirical force fields and quantum-mechanical calculations that the energy barriers for He diffusion is strongly anisotropic at temperatures below 380°C. The He diffuses most preferentially along the [001] direction, parallel to the c-axis, and could potentially explain the non-Arrhenius features noted by Reiners et al. (2002). The authors (Reich et al., 2007) calculate several effective closure temperatures by varying the activation energy (E_a), showing that by a 30% increase in E_a (using Reiners et al. 2004 calculated E_a), the closure temperature gets as high as 323°C.

5.5 Wind, Ice rafts or anthropogenic sources

Other possible sources for the contaminants could be windblown zircon grains or grains from ice rafts, and although high He ages are to be expected in East Greenland, it is unlikely that the xenocrysts were carried with ice rafts. Anthropogenic sources, contaminating the sediments in east Iceland prior to sampling, would be needed to consider. If landmass were taken from outside the island for e.g. construction, roads or other industry, this could contaminate the sediments.

5.6 Retaining helium

If the zircons extracted from the hyaloclastite and river sediment sampled in the Öræfajökull area in 2003 were actually derived from slivers of an extended JMM and the closely corresponding He/(U+Th) and U/Pb ages are correct, the following conditions must be met:

1) The extension of the JMM beneath East Iceland must be shallow enough to avoid reaching temperatures close to the blocking temperature for zircon (i.e. He).

2) The zircons must have resided within the sliver of crust until the recent basalt magmas assimilated all but the most refractory zircon grains. The time of residence in the magma before eruption must have been fairly short.

5.7 Cenozoic zircon grains

Four zircon grains from the Öræfajökull area gave older U-Pb ages than the young essentially zero-age igneous zircons. Two zircons gave an age at 30-40 Ma (DAV-13-4 383/10, SAL779 377/15), one zircon at 7.4–8.9 Ma (DAV-13-6 383/3) and the last gave an age at 4.8-5.1 Ma (DAV-13-6 383/1). There are also some U-Pb ages at ≤ 1 Ma, however, mostly with an error larger than the age (e.g. DAV-13-14 383/6). DAV-13-4 383/10 has an age of 30.8 ±3 Ma ($^{206}Pb/^{238}U$), 49.3 ±32.4 Ma ($^{207}Pb/^{235}U$) and 1081 ±951.3 Ma ($^{207}Pb/^{206}Pb$). The high uncertainty of the two latter ages (207/235 and 207/206), makes the former age of 30.8 Ma the most reliable, representing the time of crystallization. However, it is possible that the zircon is a mixture of old and new growth of Pb. Further analyses would be required to distinguish these two alternatives. One of the zircons from SAL779 yields ages of 37.0 ±3.7 Ma and 38.8 ±39.9 Ma, for ($^{206}Pb/^{238}U$) and ($^{207}Pb/^{235}U$), respectively. During the opening of the North Atlantic at about 55 Ma, the spreading occurred along the Ægir Ridge (e.g. Breivik et al., 2006). A new rift propagated north-eastwards from the Iceland plume about 30 Ma ago, leading to the formation of a new oceanic sub-basin. The two Cenozoic zircons match the age of the new rift and formation of the new sub-basin, however, it is hard to conclude where these zircons originated from. The two zircons ranging from 4.8 – 8.9 Ma (i.e. DAV-13-6 383/3 and DAV-13-6 383/1) could easily be explained as igneous zircons formed during crustal accretion in the Western Rift Zone.

5.8 Precambrian zircon grains in East Iceland: legitimate xenocrysts or contaminants?

The crushing, milling and separation of the remaining hyaloclastite tuff SAL779 and corresponding pillow-lava unit SAL768 by D.A. Valrygg, and separation of the Stigá and

Gljúfúrsá glacial river samples by F.Corfu yielded no zircon grains with an appearance similar to the previously selected Precambrian xenocrysts (e.g. SAL779 377/13 and HVRT1 377/17). To find Precambrian zircons in a sample, and then later not being able to find similar looking zircon grains by crushing and separating more of the same sample is puzzling. The failure to recover further Precambrian xenocrysts from the rest of the 2003-collected samples, as well as in the river sediments sampled by Valrygg and Corfu in 2013, raises doubt as to whether the previous findings of Precambrian xenocrysts are genuine. There have not been reports of contamination in the laboratories used for crushing, milling, washing and separation at the University of Oslo, neither before or after the processing in 2003-2004. However, one can not a priori assume that contamination during processing of the samples did not happen. The Wilfley table was used after crushing and milling of the remaining parts of SAL779 and SAL768. If any contamination happened in 2003-2004 during processing of the sample material, it might have been a single event.

One could also argue that the chance of finding xenocrystic zircons is minimal, even if quite large amounts of sample have been processed. Even though on-site heavy mineral washing was done in east Iceland, one is not guaranteed that the on-site mineral washing would be as effective as using a Wilfley table, or that the amount washed would be enough to have a statistically fair chance of finding the xenocrystic grains. Such speculations, however, do not provide any answers to the question about whether the Precambrian zircons are contamination or not.

To explain the contamination conundrum, following scenarios might be considered:

1) The zircon grains are contamination, either from the laboratory or from wind, ice or anthropogenic transport (concrete, road construction materials). The results from the current investigation of the zircons from various Precambrian and early Permian rocks from southern Norway show that the U-He ages are generally much younger than the corresponding U-Pb ages. Although similar large differences between U-He and U-Pb ages and fission tracks and U-Pb ages are evident (e.g. Rohrman et al., 1994; Hendriks et al., 2007), relatively old fission track ages have been recorded from East Greenland and in the eastern part of Scandinavia. On the basis of comparing closely corresponding U-He and U-Pb, it is only possible to conclude

where the Icelandic xenocrystic zircons do not originate from. However, to test and deduce the source of contamination based on all plausible explanations and sources one could think of would be virtually impossible.

2) The xenocrystic zircon grains are derived from an extended JMM under southeast Iceland after assimilation of crustal blocks in the recent Öræfajökull magmas. Such assimilation may have given the magmas the unique EM2-like geochemical characteristics (Torsvik et al. in preparation). All of the crustal material except for the most refractory and He-retentive zircon grains might have been assimilated in this process. Reports of such a selective survival of He-retentive Precambrian zircon crystals during magma assimilation of crustal rocks are not known to the author and the selection process remains speculative.
3) The similar U-He and U-Pb ages measured of the Precambrian xenocrystic zircons might be erroneous or a result of a lack of correction for zircon zonation. Five zircons from Iceland sampled and separated in 2003-2004 yielded U-He ages higher than their corresponding zero U-Pb ages. Two of these zircons, SB1 377/20 and SB1 377/21 with ages of 18.2 and 3.3, respectively, yielded an uncertainty of 100%. Whereas HVRT1 377/16 and SB1 377/19 yields relatively young U-He ages of 1.4 ±0.7 Ma and 1.7 ±0.34 Ma, respectively, the age of 99 ±49.5 Ma for GB1 377/22 is harder to ascribe to uncertainties. As noted previously (see results), there have been reports of a problem with blank correction, however, it is unlikely that this would result in relatively close correspondence between the U-He and U-Pb ages for the Precambrian xenocrystic zircons.

6. Conclusion

Zircons from the Öræfajökull area in East Iceland were dated by U-Pb and U-He prior to this thesis, yielding four Precambrian xenocrystic zircon grains in 2003-2004 (only U-Pb). Another four Precambrian grains with similar U-Pb and U-He ages, and one Cenozoic zircon grain were recovered from the same samples in 2013.

An effort to reproduce the results by further sampling of river sediments from a wider geographical area in the Öræfajökull area yielded very few grains that looked similar to the previously recovered Precambrian zircons. U-Pb dating of a selection of the grains that looked most promising yielded only one Cenozoic zircon and ten young igneous zircons.

A complementary investigation of zircon grains from Precambrian rocks close to and in the Oslo Rift, as well as from the Bamble complex, Telemarkia Terrane and Hardangervidda, resulted in widely different U-Pb and U-He ages. Fission track data from across Fennoscandia compiled by Hendriks et al. (2007), indicate that Precambrian rocks in Norway is predominantly reset by Caledonian and Oslo Rift tectonothermal processes, whereas areas in Finland and eastern Sweden may be largely unaffected by thermal overprinting.

Apatite fission track ages of up to 850 Ma in East Greenland (e.g. Hansen 2000), confirms that low temperature chronometers such as zircon U-He ages (in Greenland), might be as high as the ages of the Precambrian xenocrystic zircon grains from SE Iceland. If the JMM beneath Iceland was shallow enough to retain He, and the residence time for zircons in the magma was short enough, then it is possible that the previous findings of Precambrian xenocrystic zircon grains in East Iceland might reflect the assimilation of underlying continental crust.

Based on the regional variation in the U-He and fission track ages recorded by Precambrian rocks in Scandinavia and Greenland, the similar U-He and U-Pb ages for the Precambrian xenocrystic zircon grains from SE Iceland seem to exclude contamination with zircons from Norway. Although the possibility that the Precambrian xenocrysts from SE Iceland represents contamination by wind, ice or anthropogenic sources seems unlikely, this scenario cannot be excluded, either.

Precambrian zircons from the Oslo Region (i.e. Nevlunghavn and Gjersjøen) and the Bamble terrane, show abnormally high U-He ages when compared to fission track ages. This could be explained by a lack of correction for zonation, analytic problems with blank correction at SUERC and/or an underestimation of the bulk closing temperature for He diffusion. The samples from the Telemarkia terrane and Finse at Hardangervidda yields U-He ages reset by the Caledonian Orogeny, whereas the Kvitenut Nappe in Hardangervidda have not been affected by the Caledonian Orogeny to a high enough degree to reset zircon U-He ages. The orthogneiss xenolith in the larvikite in Nevlunghavn shows lead loss at c. 300 Ma, corresponding to the emplacement of the larvikite plutonic complex.

7. References

Amundsen, H.E.F.m Schaltegger, U., Jamtveit, B., Griffin, W.L., Podladchikov, Y., Torsvik, T.H. and Grönvold, K. 2002. Reading the LIP's os Iceland and Mauritius: zircon xenocrysts confirming underlying continental crust. Abstract, 25th Nordic Geological Winter Meeting, 6-9 Jan. 2002, Reykjavik, Iceland.

Andersen, T., 2005. Terrane Analysis, Regional Nomenclature and Crustal Evolution in the Southwest Scandinavian Domain of the Fennoscandian Shield. *GFF*. 127, 159-168.

Allen, R. M., Nolet, G., Morgan, W. J., Vogfjörd, K., Nettles, M., Ekström, G., Bergsson, B. H., Erlendsson, P., Foulger, G. R., Jakobsdóttir, S., Julian, B. R., Pritchard, M., Ragnarsson, S. and Stefansson, R., 2002. Plume-driven plumbing and crustal formation in Iceland. *J. Geophys. Res.* 107, 2163.

Bingen, B., Andersson, J., Söderlund, U. and Möller, C., 2008. The Mesoproterozoic in the Nordic countries. *Episodes.* 31 (1), 29-34.

Bingen, B., Nordgulen, Ø. and Viola, G. 2008. A four-phase model for the Sveconorwegian orogeny, SW Scandinavia. *Norwegian Journal of Geology*. 88, 43-72.

Breivik, A.J., Mjelde, R., Faleide, J.I. and Murai, Y. 2006. Rates of continental breakup magmatism and seafloor spreading in the Norway Basin–Iceland plume interaction. *J. geophys. Res.* 111, B07102.

Bruton, D. L., Gabrielsen, R. H. and Larsen, B. T., 2010. The Caledonides of the Oslo Region, Norway- Stratigraphy and structural elements. *Norwegian Journal of Geology.* 90 (3), 93-121.

C. W. l•AESER 1 AND I-I. FAUL 2, Fission Track Annealing in Apatite and Sphene, VOL. 74, NO. 2, JANUARY 15, 1969

Condomines, M., Gr6nvold, K., Hooker, P.J., Muehlenbachs, K., O'Nions, R.K., Oskarsson, N. and Oxburgh, E.R., 1983. Helium, oxygen, strontium and neodymium isotopic relationshipsin Icelandic volcanics. *Earth and Planetary Science Letters.* 66, 125-136.

Corfu, F., 2004. U-Pb age, setting and tectonic significance of the anorthosite-mangerite-charnockite-granite suite, Lofoten–Vesterålen, Norway. *Journal of Petrology.* 45 (9), 1799-1819.

Corfu, F., Andersen, T.B. and Gasser, D., 2014. The Scandinavian Caledonides: Main features, conceptual advances and critical questions. *Geological Society, London, Special Publications.* 390 (1), 9-43.

Corfu, F. and Dahlgren, S., 2008. Perovskite U-Pb ages and the Pb isotopic composition of alkaline volcanism initiating the Permo-Carboniferous Oslo Rift. *Earth and Planertary Science Letters.* 265 (1-2), 256-269.

Carley, T.L., Miller, C.F., Wooden, J.L., Bindeman, I.N. and Barth, A.P., 2011. Zircon from historic eruptions in Iceland: Reconstructing storage and evolution of silicic magmas. *Mineralogy and Petrology.* 102, 135-161.

Dahlgren, S., Corfu, F.,Heaman, L.M., 1996.U–Pb time constraints, and Hf and Pb source characteristics of the Larvik plutonic complex, Oslo Paleorift. Geodynamic and geochemical implications for the rift evolution. V.M. Goldschmidt Conf. J. Conf. Abstracts, vol. 120. Cambridge Publ.

Debaille, V., Trønnes, R.G., Brandon, A.D., Waight, T.E., Graham, D.W. and Lee, C.-T.A., 2009. Primitive off-rift basalts from Iceland and Jan Mayen: Os-isotopic evidence for a mantle source containing enriched subcontinental lithosphere. *Geochimica et Cosmochimica Acta.* 73, 3423-3449.

Dobson, K.J., Stuart, F.M. and Dempster, T.J., 2008. U and Th zonation in Fish Canyon Tuff zircons: Implications for a zircon (U–Th)/He standard. *Geochimica et Cosmochimica Acta.* 72 (19), 4745–4755.

Dodson, M. H. 1973. Closure temperature in cooling geochronological and petrological systems. *Contributions to Mineralogy and Petrology.* 40, 259-274.

Jensen, E. 2012. Geology and geochronology of the Hardangerjøkulen Klippe and its basement. MSc thesis, University of Oslo, 119 p.

Foeken, J.P.T., Stuart, F.M., Dobson, K.J., Persano, C. and Vilbert, D., 2006. A diode laser system for heating minerals for (U-Th)/He Chronometry. *Geochemistry, Geophysics, Geosystems.* 7 (4), Q04015.

Foulger G.R. 2002. Plumes, or plate tectonic processes?. *Astronomy & Geophysics. 43*

Foulger, G.R. 2006. Older crust underlies Iceland. *Geophys. J. Int.* **165**, 672-676.

Fossen, H., 2000. Extensional tectonics in the Caledonides: Synorogenic or postorogenic. *Tectonics*. 19 (2), 213-224.

Gaál, G. and Gorbatschev, R., 1987. An Outline of the Precambrian Evolution of the Baltic Shield. *Precambrian Research.* 35, 15-52.

Gee , D.G., Juhlin, C., Pascal, C. and Robinson, P. 2010. Collisional Orogeny in the Scandinavian Caledonides (COSC). *GFF*. 132 (1), 29-44.

Gleadow, A.J.W. and Brooks, C.K. 1979. Fission track dating, thermal histories and tectonics of igneous intrusions in East Greenland. *Contrib. Mineral. Petrol.* 71, 45– 60.

Gudmundsson, A., 2000. Dynamics of volcanic systems in Iceland: example of tectonism and volcanism at juxtaposed hot spot and mid-ocean ridge systems. *Ann. Rev. Earth Planet. Sci.* 28, 107–140.

Gudmundsson, A. 2007. Infrastructure and evolution of ocean-ridge discontinuities in Iceland. *Journal of Geodynamics*. 43. 6-29.

Gunnarsson, B., Marsh, B. D., and Taylor, H. P., 1998. Generation of Icelandic rhyolites: silicic lavas from the Torfajokull central volcano. *Journal of Volcanology and Geothermal Research.* 83, 1-45.

Gee, D.G., Fossen, H., Henriksen, N. & Higgins, A., 2008. From the early Paleozoic platforms of Baltica and Laurentia to the Caledonide Orogen of Scandinavia and Greenland. *Episodes.* 31, 44–51.

Hansen, K. and Brooks, C.K. 2002. The evolution of the East Greenland margin as revealed from fission-track studies. *Tectonphysics.* 349, 93-111.

Hansen, K. 2000. Tracking thermal history in East Greenland: an overview. *Global Planet. Change.* 24, 303–309.

Hansen, K., Brooks, C.K. 2002. The evolution of the East Greenland margin as revealed from
fission-track studies. *Tectonophysics.* 349, 93– 111.

Hardarson, B.S., Fitton, J.G., Ellam, R.M. and Pringle, M.S., 1997. Rift relocation - a geochemical and geochronological investigation of a palaeo-rift in Northwest Iceland. *Earth Planet. Sci. Lett.* 153, 181–196.

Hendriks, B.W.H. and Redfield, T.F. 2005. Apatite fission track and (U–Th)/He data from Fennoscandinavia: an example of underestimation of fission track annealing in apatite. *Earth Planet. Sci. Lett.* 236, 443–458.

Hendriks, B., Andriessen, P., Huigen, Y., Leighton, C., Redfield, T., Murrell, G., Gallagher, K. and Nielsen, S.B. 2007. A fission track data compilation for Fennoscandia. *Norwegian Journal of Geology*. 87, 143-155.

Hourigan, J., Reiners, P.W. and Brandon, M.T. 2005. U-Th zonation-dependent alpha-ejection in (U-Th)/He chronometry. *Geochimica et Cosmochimica Acta*. 69 (13), 3349–3365.

Jacoby, W. 2005. Hotspot Iceland: An introduction. *Journal of Geodynamics*. 43. 1-5

Jaffey, A. H., Flynn, K. F., Glendenin, L. E., Bentley, W. C. and Essling, A. M. 1971. Precision Measurement of Half-Lives and Specific Activities of U 235 and U 238 . *Phys. Rev*. C 4

Fossen, H., 2000. Extensional tectonics in the Caledonides: Synorogenic or postorogenic. *Tectonics*. 19 (2), 213-224.

JONASSON, K. (2007) Silicic volcanism in Iceland: Composition and distribution within the active volcanic zones. Journal of Geodynamics, 43, 101-117.

K. A. FARLEY, R. A. WOLF, and L. T. SILVER The effects of long alpha-stopping distances on (U-Th)/He ages, Division of Geological and Planetary Sciences, MS 170-25, California Institute of Technology, Pasadena, CA 91125, USA

Kaiser, A., Lobert, M. and Telle, R. Thermal stability of zircon (ZrSiO4). *Journal of the European Ceramic Society.* 28, 2199–2211.

Kokfelt, T.F., Hoernle, K., Hauff, F., Fiebig, J., Werner, R. and Garbe-Schönberg, D., 2006. Combined Trace Element and Pb-Nd–Sr-O Isotope Evidence for Recycled Oceanic Crust (Upper and Lower) in the Iceland Mantle Plume. *Journal of Petrology.* 47 (9), 1705-1749.

Kumar, P., Kind, R., Priestley, K. and Dahl-Jensen, T., 2007. Crustal structure of Iceland and Greenland from receiver function studies. *Journal of Geophysical Research B: Solid Earth.* 112 (3), B03301.

Ksienzyk, A.K., Dunkl, I., Jacobs, J., Fossen, H. and Kohlmann, F. 2014. From orogen to passive margin: constraints from fission track and (U-Th)/He analyses on Mesozoic uplift and fault reactivation in SW Norway. *Geological Society Special Publications.* 390 (1), 679-702.

Laajoki K., Corfu F. and Andersen T. 2002. Lithostratigraphy and U-Pb geochronology of the Telemark supracrustals in the Bandak-Sauland area, Telemark, South Norway. *Norwegian Journal of Geology.* 82 (3), 119-138.

Larsen, B.T., Olaussen, S., Sundvoll, B. and Heeremans, M., 2008. The Permo-Carboniferous Oslo Rift through six stages and 65 million years. *Episodes.* 31 (1), 52-58.

Larsen, B.T., Olaussen, S., Sundvoll, B. and Heeremans, M. 2007. Volcanoes and faulting in an arid climate; The Oslo Rift and North Sea in the Carboniferous and Permian, 359-251 million years ago. *In* Ramberg, I.B., Bryhni, I. and Nøttvedt, A. (eds). *The Making of a Land - Geology of Norway*. Trondheim: Geological Society of Norway, 284-327.

Larsen, G., Dugmore, A. and Newton, A., 1999. Geochemistry of historical-age silicic tephras in Iceland. *Holocene.* 9 (4), 463-471.

Lee, J.K.W., Williams, I.S. and Ellis, D.J., 1997. Pb, U and Th diffusion in natural zircon. *Nature.* 390 (6656), 159-162.

Martin, E., Sigmarsson, O., 2007. Crustal thermal state and origin of silicic magma in Iceland: the case of Torfajökull, Ljósufjöll and Snæfellsjökull volcanoes. *Contribution to Mineralogy and Petrology.* 153, 593–605.

Martin, E., Sigmarsson, O., 2010. Thirteen million years of silicic magma production in Iceland: Links between petrogenesis and tectonic settings. *Lithos 116.* 129-144

Martin, E., Paquette, J.L., Bosse, V., Ruffet, G., Tiepolo, M. and O. Sigmarsson., 2011. Geodynamic of rift–plume interaction in Iceland as constrained by new $^{40}Ar/^{39}Ar$ and in situ U–Pb zircon ages. *Earth and Planetary Science Letters.* 311, 28-38.

McGarvie, D. 2008. Rhyolitic volcano–ice interactions in Iceland. *Journal of Volcanology and Geothermal Research 185.* 367-389.

Morley, C.K., 1986.Vertical strain variations in the Osen-Røa thrust sheet, North-western Oslo Fjord, Norway. *Journal of Structural Geology.* 8 (6), 621-632.

Mittelstaedt, E., Ito, G. and Van Hunen, J., 2011. Repeat ridge jumps associated with plume-ridge interaction, melt transport, and ridge migration. *Journal of Geophysical Research-Solid Earth.* 116, 20.

Neumann, E.-R., Olsen, K.H., Baldridge, W.S. and Sundvoll, B., 1992. The Oslo Rift: A review. *Tectonophysics.* 208 (1-3), 1-18.

Norddahl, H., Ingolfsson, O., Petursson, H.G. and Hallsdottir, M. 2008. Late Weichselian and Holocene environmental history of Iceland. *Jökull. No.58*

Olaussen, S., Larsen, B.T. and Steel, R.: The Upper Carboniferous-Permian Oslo Rift; Basin Fill in Relation to Tectonic Develpoment. Pangea: Global Environments and Resources Canadian Society of Petroleum Geologists, Memoir 17, .175-197

Óskarsson, N., Sigvaldason, G.E. and Steinthórsson, S., 1982. A Dynamic Model of Rift Zone Petrogenesis and the Regional Petrology of Iceland. *Journal of Petrology.* 23, 28-74.

Paquette, L., Sigmarsson, O., Tiepolo, M., 2007. Mesozoic zircons in Miocene ignimbrite from E-Iceland: a splinter of a continental crust?. *Abstracts*, Vol. 9, 03723. SRef-ID: 1607-7962/gra/EGU2007-A-03723

PRESTVIK, T. (1985) Petrology of Quaternary volcanic rocks from Öræfi, southeast Iceland. Rep. Dept. Geol. Univ. Trondheim (Norway), 21, 81.

Pedersen, L.E., Heaman, L.M. and Holm, P.M. 1995. Further constraints on the temporal evolution of the Oslo rift from precise U–Pb zircon dating in the Siljan-Skrim area. *Lithos*. 34, 301–315.

Pedersen, R.B., Bruton, D.L. and Furnes, H. 1992. Ordovician faunas, island arcs and ophiolites in the Scandinavian Caledonides. *Terra Nova.* 4, 217-222.

Reich, M., Ewing, R.C., Ehlers, T.A. and Becker, U. 2007. Low-temperature anisotropic diffusion of helium in zircon: Implications for zircon (U–Th)/He thermochronometry. *Geochimica et Cosmochimica Acta*. 71, 3119–3130.

Reiners, P.W., Farley, K.A. and Hickes, H.J., 2002. He diffusion and (U–Th)/He thermochronometry of zircon: Initial results from Fish Canyon Tuff and Gold Butte. *Tectonophysics.* 349 (1-4) 297– 308.

Roffeis, C., Corfu, F. and Gabrielsen, R.H., 2013. A Sveconorwegian terrane boundary in the Caledonian Hardanger-Ryfylke Nappe Complex: the lost link between Telemarkia and the Western Gneiss Region? *Precambrian Research.* 228, 20– 35.

Roberts, D. and Gee, D.G. 1985. An introduction to the structure of the Scandinavian Caledonides. *In* Gee, D.G., and Sturt, B.A. (eds.) *The Caledonide Orogen – Scandinavia and Related Areas*. London: John Wiley and Sons Ltd, 55-68.

Roberts, D., 2003. The Scandinavian Caledonides: event chronology, palaeogeographic settings and likely modern analogues. *Tectonophysics.* 365 (1-4), 283– 299.

Roberts, D., Nordgulen, Ø. and Melezhik, V., 2007. The Uppermost Allochthon in the Scandinavian Caledonides: From a Laurentian ancestry through Taconian orogeny to Scandian crustal growth on Baltica. *Memoir of the Geological Society of America.* 200, 357-377.

Rohrman, M., van der Beek, P. and Andriessen, P. 1994. Syn-rift thermal structure and post-rift evolution of the Oslo Rift (southeast Norway): New constraints from fission track Thermochronology. *Earth and Planetary Science Letters*. 127 (1-4), 39-54.

Reiners, P.W., Spell, T.L., Nicolescu, S. and Zanetti, K.A. 2004. Zircon (U-Th)/He thermochronometry: He diffusion and comparisons with 40Ar/39Ar dating. *Geochimica et Cosmochimica Acta*. 68 (8), 1857–1887.

Reiners, P. W. and Farley, K.A. 1999. Helium diffusion and (U-Th)/He thermochronometry of titanite. *Geochimica et Cosmochimica Acta*. 63, 3845–3859.

Saunders, A.D., Fitton, J.G., Kerr, A.C., Norry, M.J. and Kent, R.W. 1997. The North Atlantic Igneous Province. In: Mahoney, J.J., Coffin, M.F.(Eds.), Large Igneous Provinces: Continental, Oceanic, and Planetary Flood Volcanism. Geophys. Monogr. 100. American Geophysical Union,Washington, DC, pp. 45–93.

Sharma, K., Self, S., Blake, S., Thordarson, T. and Larsen, G., 2008. The AD 1362 Öræfajökull eruption, S.E. Iceland: Physical volcanology and volatile release. *Journal of Volcanology and Geothermal Research.* 178 (4), 719–739.

Sigmarsson, O., Condomines, M. and Fourcade, S. 1992. Mantle and crustal contribution in the genesis of Recent basalts from off-rift zones in Iceland: Constraints from Th, Sr and O isotopes. *Earth and Planetary Science Letters.* 110. 149-162.

Stacey, J.S. and Kramers, J.D., 1975. Approximation of terrestrial lead isotope evolution by a two-stage model. *Earth and Planetary Science Letters.* 26 (2), 207-221.

Steiger, R.H. and Jäger, E., 1977. Subcommission on Geochronology: Convention on the Use
of Decay Constants in Geo- and Cosmochronology. *Earth and Planetary Sctence Letters.* 36 (3), 359-362.

Stevenson, J.A., McGarvie, D.W., 2006. Subglacial and ice-contact volcanism at the Öræfajökull stratovolcano, Iceland. *Bull Volcanol.* 68, 737-752.

Tagami, T., Farley, K.A. and Stockli, D.F. 2003. (U^Th)/He geochronology of single zircon grains of known Tertiary eruption age. *Earth and Planetary Science Letters.* 207 (1-4), 57-67.

THORARINSSON, S. (1958) The Öræfajökull Eruption of 1362. *Acta Naturalia Islandica*, II (2).

Thordarson, T. and Larsen, G., 2007., Volcanism in Iceland in historical time: Volcano types, eruption styles and eruptive history. *Journal of Geodynamics.* 43, 118-152.

Torsvik, T.H., Amundsen, H., Hartz, E.H., Corfu, F., Kusznir, N., Gaina, C., Doubrovine, P.V., Steinberger, B., Ashwal, L.D. and Jamtveit, B., 2013. A Precambrian microcontinent in the Indian Ocean. *Nature Geoscience.* 6 (3), 223-227.

Torsvik, T.H., Smethurst, M.A., Burke, K. and Steinberger, B., 2008. Long term stability in deep mantle structure: Evidence from the ~300 Ma Skagerrak-Centered Large Igneous Province (the SCLIP). *Earth and Planertary Science Letters.* 267 (3-4), 444-452.

Torsvik, T. H., Mosar, J. and Eide, E. A., 2001. Cretaceous-Tertiary geodynamics: a North Atlantic exercise. *Geophysical Journal International.* 146, 850-866.

Walker, A.J., 2011. RHYOLITE VOLCANISM AT ÖRÆFAJÖKULL VOLCANO, S.E. ICELAND – A WINDOW ON QUATERNARY CLIMATE CHANGE. *PhD*

Zahid A. 2000. Geochronology and evolution of the Precambrian Gjersjø dome, SE-Norway. Cand. Scient. Thesis, University of Oslo, 68p.

Zaun, P. and Wagner, G.A. 1985. Fission track stability in zircons under geological conditions. *Nucl. Tracks Radiat. Meas.* 10, 303-307.